



ESCUELA TÉCNICA SUPERIOR DE INGENIERÍA (ICAI)
INGENIERO ELECTROMECAÁNICO

DISEÑO DE UN CARGADOR DE BATERÍAS

Autor: Antonio Pérez-Coca López
Director: Mahesh Krishnamurthy

Madrid
Julio 2016

Antonio
Pérez-Coca
López

DISEÑO DE UN CARGADOR DE BATERÍAS



AUTORIZACIÓN PARA LA DIGITALIZACIÓN, DEPÓSITO Y DIVULGACIÓN EN RED DE PROYECTOS FIN DE GRADO, FIN DE MÁSTER, TESINAS O MEMORIAS DE BACHILLERATO

1º. Declaración de la autoría y acreditación de la misma.

El autor D. ANTONIO PÉREZ-COCA LÓPEZ DECLARA ser el titular de los derechos de propiedad intelectual de la obra: DISEÑO DE UN CARGADOR DE BATERÍAS, que ésta es una obra original, y que ostenta la condición de autor en el sentido que otorga la Ley de Propiedad Intelectual.

2º. Objeto y fines de la cesión.

Con el fin de dar la máxima difusión a la obra citada a través del Repositorio institucional de la Universidad, el autor **CEDE** a la Universidad Pontificia Comillas, de forma gratuita y no exclusiva, por el máximo plazo legal y con ámbito universal, los derechos de digitalización, de archivo, de reproducción, de distribución y de comunicación pública, incluido el derecho de puesta a disposición electrónica, tal y como se describen en la Ley de Propiedad Intelectual. El derecho de transformación se cede a los únicos efectos de lo dispuesto en la letra a) del apartado siguiente.

3º. Condiciones de la cesión y acceso

Sin perjuicio de la titularidad de la obra, que sigue correspondiendo a su autor, la cesión de derechos contemplada en esta licencia habilita para:

- a) Transformarla con el fin de adaptarla a cualquier tecnología que permita incorporarla a internet y hacerla accesible; incorporar metadatos para realizar el registro de la obra e incorporar “marcas de agua” o cualquier otro sistema de seguridad o de protección.
- b) Reproducir la en un soporte digital para su incorporación a una base de datos electrónica, incluyendo el derecho de reproducir y almacenar la obra en servidores, a los efectos de garantizar su seguridad, conservación y preservar el formato.
- c) Comunicarla, por defecto, a través de un archivo institucional abierto, accesible de modo libre y gratuito a través de internet.
- d) Cualquier otra forma de acceso (restringido, embargado, cerrado) deberá solicitarse expresamente y obedecer a causas justificadas.
- e) Asignar por defecto a estos trabajos una licencia Creative Commons.
- f) Asignar por defecto a estos trabajos un HANDLE (URL *persistente*).

4º. Derechos del autor.

El autor, en tanto que titular de una obra tiene derecho a:

- a) Que la Universidad identifique claramente su nombre como autor de la misma
- b) Comunicar y dar publicidad a la obra en la versión que ceda y en otras posteriores a través de cualquier medio.
- c) Solicitar la retirada de la obra del repositorio por causa justificada.
- d) Recibir notificación fehaciente de cualquier reclamación que puedan formular terceras personas en relación con la obra y, en particular, de reclamaciones relativas a los derechos de propiedad intelectual sobre ella.

5º. Deberes del autor.

El autor se compromete a:

- a) Garantizar que el compromiso que adquiere mediante el presente escrito no infringe ningún derecho de terceros, ya sean de propiedad industrial, intelectual o cualquier otro.
- b) Garantizar que el contenido de las obras no atenta contra los derechos al honor, a la intimidad y a la imagen de terceros.
- c) Asumir toda reclamación o responsabilidad, incluyendo las indemnizaciones por daños, que pudieran ejercitarse contra la Universidad por terceros que vieran infringidos sus derechos e

intereses a causa de la cesión.

- d) Asumir la responsabilidad en el caso de que las instituciones fueran condenadas por infracción de derechos derivada de las obras objeto de la cesión.

6º. Fines y funcionamiento del Repositorio Institucional.

La obra se pondrá a disposición de los usuarios para que hagan de ella un uso justo y respetuoso con los derechos del autor, según lo permitido por la legislación aplicable, y con fines de estudio, investigación, o cualquier otro fin lícito. Con dicha finalidad, la Universidad asume los siguientes deberes y se reserva las siguientes facultades:

- La Universidad informará a los usuarios del archivo sobre los usos permitidos, y no garantiza ni asume responsabilidad alguna por otras formas en que los usuarios hagan un uso posterior de las obras no conforme con la legislación vigente. El uso posterior, más allá de la copia privada, requerirá que se cite la fuente y se reconozca la autoría, que no se obtenga beneficio comercial, y que no se realicen obras derivadas.
- La Universidad no revisará el contenido de las obras, que en todo caso permanecerá bajo la responsabilidad exclusiva del autor y no estará obligada a ejercitar acciones legales en nombre del autor en el supuesto de infracciones a derechos de propiedad intelectual derivados del depósito y archivo de las obras. El autor renuncia a cualquier reclamación frente a la Universidad por las formas no ajustadas a la legislación vigente en que los usuarios hagan uso de las obras.
- La Universidad adoptará las medidas necesarias para la preservación de la obra en un futuro.
- La Universidad se reserva la facultad de retirar la obra, previa notificación al autor, en supuestos suficientemente justificados, o en caso de reclamaciones de terceros.

Madrid, a 18 de julio de 2016

ACEPTA

Fdo: Antonio Pérez-Coca López

Motivos para solicitar el acceso restringido, cerrado o embargado del trabajo en el Repositorio Institucional:

Declaro, bajo mi responsabilidad, que el Proyecto presentado con el título
DISEÑO DE UN CARGADOR DE BATERÍAS
en la ETS de Ingeniería - ICAI de la Universidad Pontificia Comillas en el
curso académico 2015/2016 es de mi autoría, original e inédito y
no ha sido presentado con anterioridad a otros efectos. El Proyecto no es
plagio de otro, ni total ni parcialmente y la información que ha sido tomada
de otros documentos está debidamente referenciada.

Fdo.: Antonio Pérez-Coca López

Fecha: 19/07/2016

Autorizada la entrega del proyecto

EL DIRECTOR DEL PROYECTO

Fdo.: Mahesh Krishnamurthy

Fecha: 19/07/2016

Vº Bº del Coordinador de Proyectos

Fdo.: Álvaro Sánchez Miralles

Fecha: 19/07/2016



ESCUELA TÉCNICA SUPERIOR DE INGENIERÍA (ICAI)
INGENIERO ELECTROMECAÁNICO

DISEÑO DE UN CARGADOR DE BATERÍAS

Autor: Antonio Pérez-Coca López
Director: Mahesh Krishnamurthy

Madrid
Julio 2016

Antonio
Pérez-Coca
López

DISEÑO DE UN CARGADOR DE BATERÍAS



INDEX

Chapter 1: Introduction	9
1.1- Present-day context	9
1.2- State of the art	10
1.3- Motivation	16
1.4- Objectives and methodology	17
1.5- Resources	17
Chapter 2: Design of the circuit.....	19
2.1- The battery	19
2.2- The charging method.....	20
2.3- The circuit	23
2.3-1. The battery model	25
2.3-2. The AC power source	29
2.3-3. The full wave rectifier.....	29
2.3-3.1. Drawbacks of this rectifier	33
2.3-4. Power factor correction (PFC)	34
2.3-4.1. Design considerations	36
2.3-4.2. Design of the components.....	37
2.3-4.3. Controlling the PFC	38
2.3-5. The buck converter	40
2.3-5.1. Design considerations	42
2.3-5.2. Design of the components.....	43
2.3-5.3. Controlling the buck converter	46
2.3-6. The input inductor	57
2.4- The resulting battery charger.....	58

UNIVERSIDAD PONTIFICIA COMILLAS
ESCUELA TÉCNICA SUPERIOR DE INGENIERÍA (ICAI)
INGENIERO ELECTROMECAÁNICO

Chapter 3: Components	59
2.5- Transistors	59
2.6- Diodes	61
2.7- Inductors	63
2.8- Capacitors	63
2.9- Microcontroller	65
Chapter 4: Costs.....	67
Chapter 5: Simulations and remarks.....	69
Chapter 6: Power efficiency	85
Chapter 7: Conclusion.....	87
Chapter 8: Future developments.....	91
Chapter 9: References	93

FIGURES INDEX

Figure 1: NiCd rechargeable batteries	10
Figure 2: NiMH rechargeable batteries.....	11
Figure 3: Lithium Ion batteries	11
Figure 4: NDV and dT/dt termination methods.....	13
Figure 5: Voltage and current curves of a Li-Ion battery (CC-CV)	14
Figure 6: AllCell HE-4820 Li-Ion battery	19
Figure 7: battery model.....	20
Figure 8: CC-CV flowchart diagram	22
Figure 9: CC-CV voltage and current curves	23
Figure 10: Block diagram with the sub-circuits of the battery charger	24
Figure 11: Discharge curves for the LG Li-Ion cell under different C-rates	27
Figure 12: Simple discharge circuit	28
Figure 13: Battery model discharge curves	28
Figure 14: AC power source.....	29
Figure 15: Bridge rectifier	29
Figure 16: Bridge rectifier's modes of operation.....	30
Figure 17: Bridge rectifier's input (red) and output (blue) voltage waveforms.	31
Figure 18: Bridge rectifier with smoothing capacitor.....	32
Figure 19: Bridge rectifier's input (red) and output (blue) voltage waveforms with the smoothing capacitor.....	33
Figure 20: Input voltage (blue) and current (waveforms).....	34
Figure 21: Class D voltage and required current waveform.	35
Figure 22: Class A voltage and admissible current waveform.	35
Figure 23: Topology for both the bridge rectifier and the PFC.	36
Figure 24: PFC inner and outer control loops.....	39

UNIVERSIDAD PONTIFICIA COMILLAS
 ESCUELA TÉCNICA SUPERIOR DE INGENIERÍA (ICAI)
 INGENIERO ELECTROMECAÁNICO

Figure 25: Basic switching converter and its output voltage.	41
Figure 26: (a) Buck dc-dc converter; (b) Equivalent circuit for the switch closed; (c) Equivalent circuit for the switch open.	42
Figure 27: Flowchart diagram of the CC-CV process executed by the buck converter's controls.....	46
Figure 28: Buck converter topology with feedback loop.....	48
Figure 29: Nichols chart and step response of the resulting controlled system.....	50
Figure 30: Diagram for the PWM modulator.	51
Figure 31: Buck converter's voltage control circuit implemented in PSIM.....	51
Figure 32: Buck converter's voltage control circuit implemented in PSIM.....	52
Figure 33: Voltage waveform showing the problem caused when switching from CC to CV.....	54
Figure 34: Hysteresis comparator.	54
Figure 35: Hysteresis comparator's waveforms.	55
Figure 36: Charge termination control.....	56
Figure 37: Signal's multiplexor	56
Figure 38: Complete circuit	58
Figure 39: Comparison between MOSFETs and IGBTs.....	60
Figure 40: IRFP460 Power MOSFET.....	61
Figure 41: Fairchild Semiconductor FFPF20UP40S	62
Figure 42: Selected bridge rectifier.....	62
Figure 43: Designed inductor.....	63
Figure 44:United Chemicon aluminum electrolytic capacitor.....	64
Figure 45: Input voltage and current to the final charger before applying the PFC.	70
Figure 46: Above: Input voltage and current to the charger using PFC. Below: PFC's output voltage.	71
Figure 47: PFC topology with its feedback loop.	72
Figure 48: PFC controls' simulations.....	73
Figure 49: PFC controls' simulations.....	74

UNIVERSIDAD PONTIFICIA COMILLAS
ESCUELA TÉCNICA SUPERIOR DE INGENIERÍA (ICAI)
INGENIERO ELECTROMECAÁNICO

Figure 50: PFC's PWM signal.	75
Figure 51: a) PFC's output voltage. b) Buck converter's output voltage. c) Buck converter's output current.	76
Figure 52: Buck converter's control's signals in CC.	77
Figure 53: Buck converter's control's signals in CV.	78
Figure 54: Results of the voltage and current charging curves.	79
Figure 55: Charging curves for an LG battery cell under several C-rates.	80
Figure 56: Battery voltage and current curves at SOC=0.1.	82
Figure 57: Battery voltage and current curves at SOC=0.95.	83
Figure 58: End of charge battery voltage, current and SOC.	84

TABLES INDEX

Table 1: AllCell HE-4820 specifications.	20
Table 2: Parameters introduced in the Li-Ion battery model.	26
Table 3: Specifications for the PFC design.	37
Table 4: Multiplexor's table of truth.	56
Table 5: Comparison between IGBTs and MOSFETs.	61
Table 6: Specifications for the microcontroller.	65
Table 7: Components and costs.	68

UNIVERSIDAD PONTIFICIA COMILLAS
ESCUELA TÉCNICA SUPERIOR DE INGENIERÍA (ICAI)
INGENIERO ELECTROMECAÁNICO

UNIVERSIDAD PONTIFICIA COMILLAS
ESCUELA TÉCNICA SUPERIOR DE INGENIERÍA (ICAI)
INGENIERO ELECTROMECAÁNICO

MEMORIA

UNIVERSIDAD PONTIFICIA COMILLAS
ESCUELA TÉCNICA SUPERIOR DE INGENIERÍA (ICAI)
INGENIERO ELECTROMECAÁNICO

Chapter 1: Introduction

In this first chapter, an introduction to the present project will be done. Section 1.1 briefly explains the present-day context concerning rechargeable batteries. Section 1.2 explains the available technologies used for charging such batteries, which will lead to the motivation of the present project, presented in section 1.3. Section 1.4 will explain in more detail the objectives pursued in this project and finally sections 1.5 and 1.6 will explain the methodology and resources used for achieving those objectives.

1.1- Present-day context

From the not so popular electric toothbrush to the ubiquitous cell phone, and from the small earpiece to the satellites in orbit, the variety of devices and machines powered by rechargeable batteries is enormous, and rapidly increasing. Devices that are used on a daily basis and therefore need frequent recharges. This technologic field is therefore very promising, with great developments that are yet to come.

The sector is divided in two main branches: improving the efficiency of the devices to make them less energy consuming, and developing better batteries.

The second branch is the one of interest in this project, and it is as well divided in two main areas: the actual battery and the device used to recharge it. Improving the battery itself means finding better chemistries and architectures which will expand the number of charging cycles, increase the capacity and energy density, reduce size and costs, etc. Concerning the battery chargers, the aim is to achieve devices with greater efficiency and performance, being able to charge the battery as fast as possible without compromising accuracy or safety.

This technology is already quite advanced, but users keep finding problems when using it (burnt batteries, slow charge at low or high temperatures, etc), so there is still much room for improvements. Furthermore, new technologies such as electric vehicles and their so-called

superchargers keep pushing the battery charger technology forward at a very fast rate, making it a very interesting area of engineering.

There are many types of battery chemistries used in the industry (Nickel Cadmium NiCd, Nickel-Metal Hydride NiMH, Lead Acid, Lithium Ion, Lithium Polymer, etc), and each one of them has its own requirements and limitations in terms of how they get charged. Even in a single chemistry there are several solutions and charging methods that could be used. All of them are charged by forcing an electric current into the battery, but this may be done in many different ways and with different levels of accuracy and control.

From all the mentioned battery chemistries, the most widely used is the Lithium Ion battery, which is the one found in devices such as cell phones, cameras, laptops, and even electric vehicles. It has therefore been the preferred one for the battery charger design proposed in this project.

1.2- State of the art

As it was mentioned before, in the market there are several types of battery chemistries, each one with their advantages and limitations. First, a short description of the three of the most important chemistries (NiCd, NiMH and Li-Ion) will be presented [15], followed by the different charging methods used in these battery types. The battery chemistries:

- **Nickel Cadmium (NiCd):** this “classic” battery type has been around for a long time (the first nickel-cadmium battery cell was invented in 1899) and it is therefore a well known and developed product. With a cycle durability of 2,000 cycles, an energy density of 50 to 150 Wh/L and a low price, this type of battery is mainly used in applications where long life and economical price are important. These applications include biomedical equipment, professional photography equipment, flashlights and



Figure 1: NiCd rechargeable batteries

many more. However, this chemistry contains toxic materials and it has a very low energy density.

- **Nickel-Metal Hydride (NiMH):** until the mid-1990s, the main battery chemistry in the market was the NiCd battery, but due to its limitations (low energy density) and disadvantages (toxic metals) it was rapidly substituted by the NiMH. This type of battery can have as much as three times the capacity of a NiCd battery having the same size, and it does not contain any environmentally unfriendly elements. It's cycle durability ranges from 500 to 2000 cycles and its energy density goes from 140 to 300 Wh/L. Due to this advantages, this chemistry has replaced the NiCd battery in many applications in consumer electronics and it has been widely used in electric vehicles.



Figure 2: NiMH rechargeable batteries

- **Lithium Ion (Li-ion):** after an exponential growth over the last few decades [16], the Li-Ion battery is today the most widely used chemistry in portable applications such as laptops or cell phones. This is for many reasons that will be explained in detail later in the project, but mainly due to its high energy density (250 to 676 Wh/L) and its lightweight. Nevertheless, this chemistry is quite fragile and charging it requires great accuracy to assure its safety. Figure 3 shows the Li-Ion battery cells that compose the battery pack used in the design of the present project.



Figure 3: Lithium Ion batteries

UNIVERSIDAD PONTIFICIA COMILLAS
ESCUELA TÉCNICA SUPERIOR DE INGENIERÍA (ICAI)
INGENIERO ELECTROMECAÁNICO

Now that the main battery chemistries have been introduced, this section continues with the charging methods used for recharging these batteries. In most battery chemistries, chargers are usually divided in two big blocks: slow chargers and fast chargers.

- **Slow chargers:** also known as trickle current, this charging method consists of applying a very low charging current (around $0.1C$) that can be applied to the battery indefinitely without causing any harm to the battery.

The problem of continued charging after the battery is fully charged is that the energy can no longer be stored and it starts a process of liberating gas inside the battery cells. If the pressure reaches a certain limit, internal vents will have to open to release the gas. This causes harm to the battery since that gas will leave the battery forever and this will decrease the life of the cell.

The advantage of this type of chargers is that the rate of charge is so small that the liberated gas is able to recombine internally, without having to be released. But nevertheless, once the battery is fully charged it should be disconnected to prolong the battery lifetime. Some chemistries like NiCd respond well to trickle charging because its fast recombination keeps the cell voltage at a safe level. Nevertheless, the pressure inside the battery is high enough to produce some gas leaks, so it is better to disconnect the battery once it is charged.

Other chemistries like NiMH end up getting damaged if charged with trickle current for too long. And finally Li-Ion batteries cannot tolerate this type of chargers because they are very sensitive to overcharging.

In conclusion, the greatest advantage of this charging method is that since it virtually cannot cause any harm to the battery by charging it at such a slow rate, the charger does not need a system to detect and cut the charging when it is complete, which exponentially reduces the complexity and price of the charger.

On the other hand, the greatest disadvantage is the time it takes to fully charge the battery. It can take a whole overnight charge or even longer, and for many applications

this is too long. The consumer wouldn't buy a charger that takes 14 to 16 hours to charge its cell phone.

- **Fast charge:** This type of charger also delivers a constant current but it does so at a much higher rate, usually 1.2C for NiCd and NiMH, reaching recharge times of 1 hour. However, increasing the charging rate also increases the chances of damaging the battery by overcharging or overheating it. Therefore, it is essential for this type of charger to have one or several charge termination methods to disconnect the battery if it is fully charged or if it surpasses a temperature limit that could harm it. The termination method will depend on the battery chemistry: some of them are more liable to overheating, some others cannot accept overcharge. This makes each charger generally suitable only for the battery type it was designed for, and trying to charge another type of battery could damage it.

There are several termination methods [17]:

- Negative delta V (NDV): this is one of the most popular methods for terminating charge. Many battery chemistries but especially NiCd batteries have their voltages increase as they are being charged, and when they are fully charged, the voltage starts decreasing. What this method does is detect when this happens and immediately cut-off the charge. This is most effective in NiCd batteries since this change in the slope of the voltage curve is very easy to detect. Figure 4 shows the charge curve for NiMH and NiCd. It also shows the temperature curve, which will be essential for the next termination method.

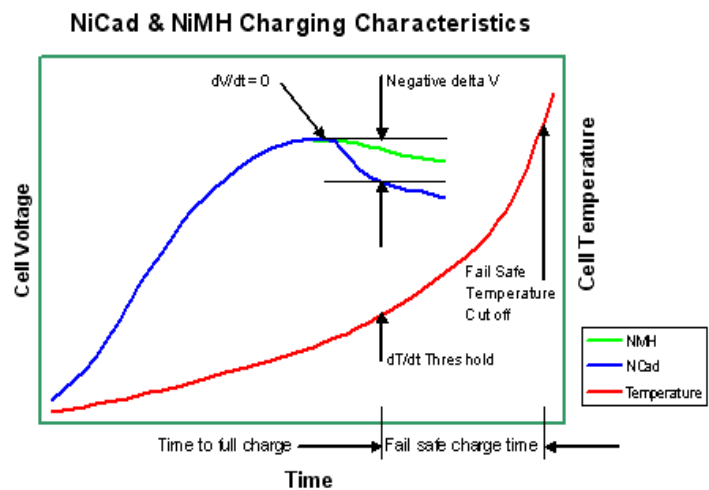


Figure 4: NDV and dT/dt termination methods

- dT/dt temperature control: some battery chemistries like NiMH do not have such a pronounced change in the slope of the voltage curve when fully charged. Therefore, using the NDV method is not reliable. Instead, the rate at which the cell temperature rises is measured, and once the rate surpasses a specified limit (the one related to full charge), the charger stops the fast charge and either disconnects the battery from the power source or changes to trickle current to finish the charge process with more accuracy.

- Constant Current Constant Voltage (CC-CV) method: this method is mainly used for Lithium Ion batteries but it is also used in other chemistries which are sensitive to overcharge. This method consists of two stages: during the first one, the charger delivers a constant current and this makes the battery voltage slowly increase. The value for the charge current is usually specified by the battery manufacturer. Then, when the battery reaches its maximum voltage and before this limit is surpassed, the charger changes to the second stage and starts controlling the battery voltage to keep it at the maximum value. During this stage, the current will start to decrease, and once it falls to a certain value (around 10% of the charge current), the charger will terminate the charge. Figure 5 shows the voltage and current curves when the battery is charged using this method.

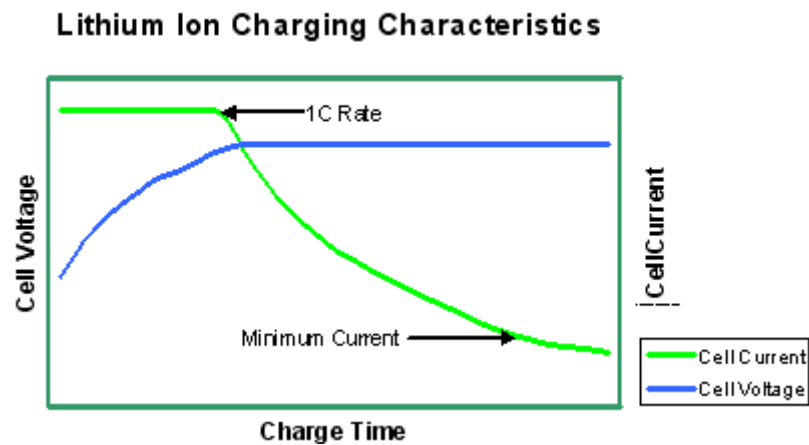


Figure 5: Voltage and current curves of a Li-Ion battery (CC-CV)

After introducing the main types of battery charging methods, it is also important to distinguish the different ways in which the battery controls the level of current or voltage to deliver to the battery. There are three main types of charge circuit technology, each with its advantages and trade-offs concerning efficiency, cost, size and simplicity:

- **Linear regulator:** This is the simplest topology, and it consists of a high power transistor used in the linear region, whose voltage drop is the difference between the input voltage and the voltage applied to the battery. This obviously consumes a lot of energy, having low efficiency, and it produces a lot of heat due to the Joule effect. Since there is no switching, the output voltage is pure dc and there is no noise generated. Another advantage is that since it does not have many components it has a small size. This topology is the preferred for applications where low noise is important such as radios.

- **Pulsed charger:** during the first low-voltage stage, this type of charger works essentially the same way as a linear regulator, with a linear transistor. But as the battery reaches its maximum voltage, the charging method changes and the transistor starts being used as a switch, delivering pulses of increasing charge current. This method permits the battery to stabilize during the rest periods between pulses, making it a safer method. The fact that they are not linear during the whole process makes the losses decrease, but this type of charger needs current limiting on the input which makes the price increase.

- **Switch mode regulator:** this type of charger use a transistor as a switch, being controlled with pulsed width modulation (PWM) to maintain the current or voltage at a desired value. This type of battery charger has the lowest heat dissipation and is therefore the most efficient type. The only problems with this topology are its size

(they need more components such as a big LC output filter to deliver dc, making the device bigger than the two preceding types), and it is the most complex topology, needing very accurate current and voltage controls to perform the CC-CV charging method.

1.3- Motivation

After having learned about the market of rechargeable batteries and their chargers, it is clear that it is a very promising technologic field, due to its immense demand and the many advances that are yet to come. From the most advanced cell phones to the electric vehicle's superchargers, it is a very interesting sector for engineers who want to participate in the research and progress of cutting edge technology.

Electronic portable devices are part of our daily lives, and it is this popularity which makes the improvement of this technology so important. Everyone charges their cell phone on a daily basis and in a few years from now electric vehicles will be everywhere. It is therefore crucial to develop a technology with the highest efficiency possible; if the designer is able to make a circuit that saves 1 watt per charger every day, globally this will mean whole megawatts saved.

For this reason, this project presents the design of a Lithium Ion battery charger, the most used in the electronic portable devices nowadays. The chosen charging method will be Constant Current Constant Voltage, because despite its complexity it is the safest method for charging this type of battery. With this purpose, a switch mode regulator will be designed to guarantee the highest efficiency.

1.4- Objectives and methodology

The proposed circuit has to be able to charge the battery using the CC-CV charging method, being powered by a normal $120/220V_{\text{rms}}$ and 60/50Hz AC power plug, and also complying with the power factor regulations, which are very stringent in this type of devices. In order to achieve this, the following sub-circuits will be designed and integrated to compose the final battery charger:

- Design of a battery model after an AllCell 48V 1000W battery pack.
- Ac to dc rectifier to convert the power received from the outlet.
- Power factor corrector (PFC) to achieve the required power factor of 1.
- Dc-dc buck converter to step down the dc voltage delivered by the PFC and to control the current and voltage levels required for safely charging the battery.
- Finally, the design of the feedback loop controls for both the PFC and the buck converter to guarantee the correct functioning of the battery charger.

After all this elements have been designed and successfully integrated with each other, the whole system will be simulated to verify that it has been correctly designed and that the battery charges with the expected voltage and current curves.

Finally, if the plan goes as expected and time permits it, a prototype for the designed circuit will be created.

1.5- Resources

The battery charger circuit was designed and simulated using PSIM, an electronic simulation software developed by Powersim. It is a powerful software which permits the user design electronic circuits in a very intuitive and complete way, being able to model real components to make the simulations as accurate as possible.

MATLAB was also used in the stage of the project related to the feedback loop designs.

UNIVERSIDAD PONTIFICIA COMILLAS
ESCUELA TÉCNICA SUPERIOR DE INGENIERÍA (ICAI)
INGENIERO ELECTROMECAÁNICO

Chapter 2: Design of the circuit

2.1- The battery

In the market of portable electronics devices, there are many types of rechargeable batteries: lead-acid, nickel-metal hydride (NiMH), nickel-cadmium (NiCd), lithium-ion polymer (Li-ion polymer) and lithium-ion (Li-ion). For this project, the battery charger was designed for a lithium ion battery. This is because it is the most extensively used technology in portable electronics due to its numerous advantages:

- High energy density: the higher the energy density the longer the battery runtime will be.
- No memory effect: some batteries tend to gradually lose capacity if they are repeatedly recharged without being completely discharged before.
- High operation voltage
- Low self-discharge: even if the battery is not connected and delivering current, rechargeable batteries tend to self-discharge. In Li-Ion batteries this happens at a rate of 1.5-2% per month.

This makes Li-ion batteries the most used and promising. They are widely used not only in consumer electronics (mobile phones, laptops and tablets, digital cameras, etc), but also in electric vehicles and military and aerospace appliances.



Figure 6: AllCell HE-4820 Li-Ion battery

The battery chosen for the design of this charger is an AllCell HE-4820 (Figure 6), and has the following specifications:

Specifications	HE-4820
Nominal Voltage	48V
Capacity Nominal (Rated)	20.8Ah (19.5Ah)
Nominal Energy	1000Wh
Operating Voltage	54.6 ~ 40V
Maximum Charge Current	10A
Temperature Range	-20° to 60°C

Table 1: AllCell HE-4820 specifications

2.2- The charging method.

Without delving too much into the battery chemistry, it is interesting to understand how the process of charge and discharge happens. When batteries are being used, the lithium ions (Li^+) make the current flow from the negative to the positive electrode. In order to charge it, an over-voltage (a higher voltage than the one produced by the battery, with the same polarity) must be applied to make the current go in the reverse direction.

There are two parameters that are important during the

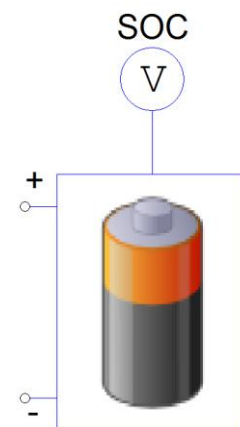


Figure 7: battery model

charging process of the battery:

- 1- The state of charge, known as SOC, refers to the available capacity in the battery, expressed as a percentage. This can be used as an indication of the time the battery has left while discharging, or as a measure of how charged the battery is during the charging process.

In the PSIM battery model, this parameter is measured using a voltmeter connected to the top pin, as shown in Figure 7. It ranges from 0 (fully depleted) to 1 (fully charged).

However, in real batteries, this parameter cannot be measured directly (see Appendix A for the different methods used in measuring SOC).

- 2- The rate of charge, known as C-rate, expresses the current at which the battery charges or discharges in relation to the capacity of the battery. It is defined as $I = M \cdot C_n$, where I is the current (in A), M is a fraction of C, C_n is the capacity of the battery expressed in Ah (ampere-hour), and n is the number of hours at which C is declared. For example, if the battery is being discharged at a rate of 1C, it will deliver its rated capacity in 1 hour.

For charging the Li-Ion battery, the preferred method is called constant current – constant voltage (CC-CV). This method consists of three stages:

- 1- Trickle charge: due to the memory effect, some batteries like NiCd must be completely discharged before being charged. Li-Ion batteries do not suffer this, and therefore can be charged at any SOC without losing capacity. Nevertheless, if the battery cell is below 2.5V, it should be charged at a maximum rate of 0.1C until it reaches 3V. In the AllCell battery, if the output voltage is below 33V, it should be charged with a current of 1A until it reaches 39V.

However, this stage is rarely used in Li-Ion chargers. Moreover, the PSIM battery model is very simple and the cells never go below 3V, being this first stage unnecessary in the designed charger.

- 2- Constant current (CC): during this stage, the charger supplies a constant current to the battery, usually between 0.2C and 1C. The recommended charging current in the AllCell

battery is 10A, which is 0.5C. During this stage, the current will be controlled and kept steady as the voltage rises. Once this voltage reaches its maximum value (54.6V in the AllCell battery, 4.2V per cell) the system will switch to the next charging stage.

- 3- Constant voltage (CV): in this final stage, the charger applies a constant voltage equal to the maximum voltage of the battery (in this case 54.6V, 4.2V per cell). The current will gradually decline, and when it reaches around 3% (in this case 1A) of the rated charge current the battery will be charged and the process will be stopped.

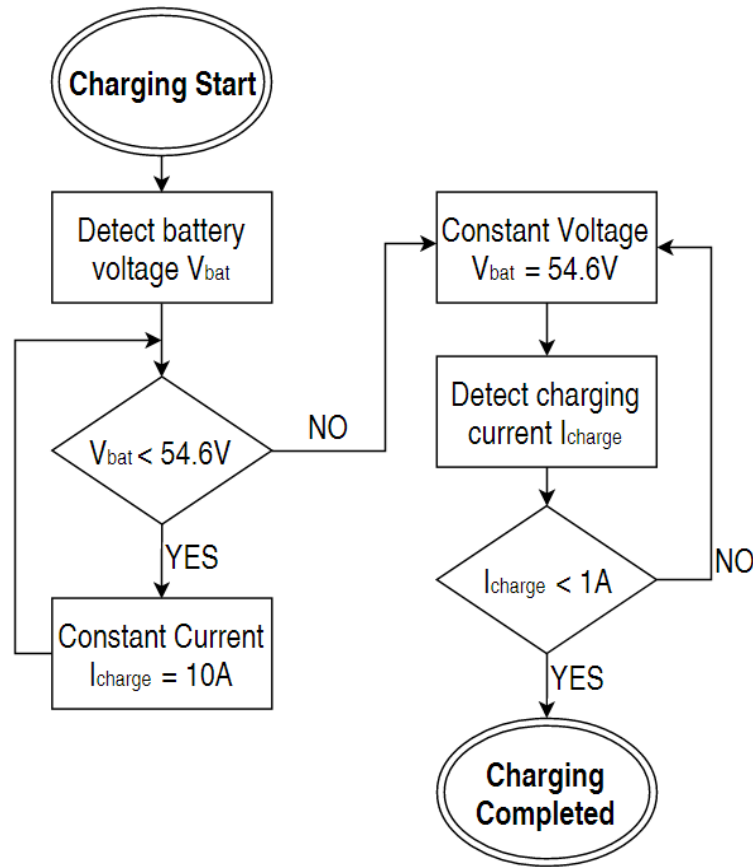


Figure 8: CC-CV flowchart diagram

Figure 8 shows a flowchart diagram of this process. It will take approximately 2.5 hours. Although increasing the current in the CC stage will make it possible to accelerate the process at the beginning (it will arrive to about 70% faster), the total charge time will remain more or less

the same. The shorter the CC stage, the longer the CV stage will be. Therefore, a charge current of 10A was selected, as it was recommended by manufacturers. Figure 9 shows what the voltage and current curves will look like throughout the process.

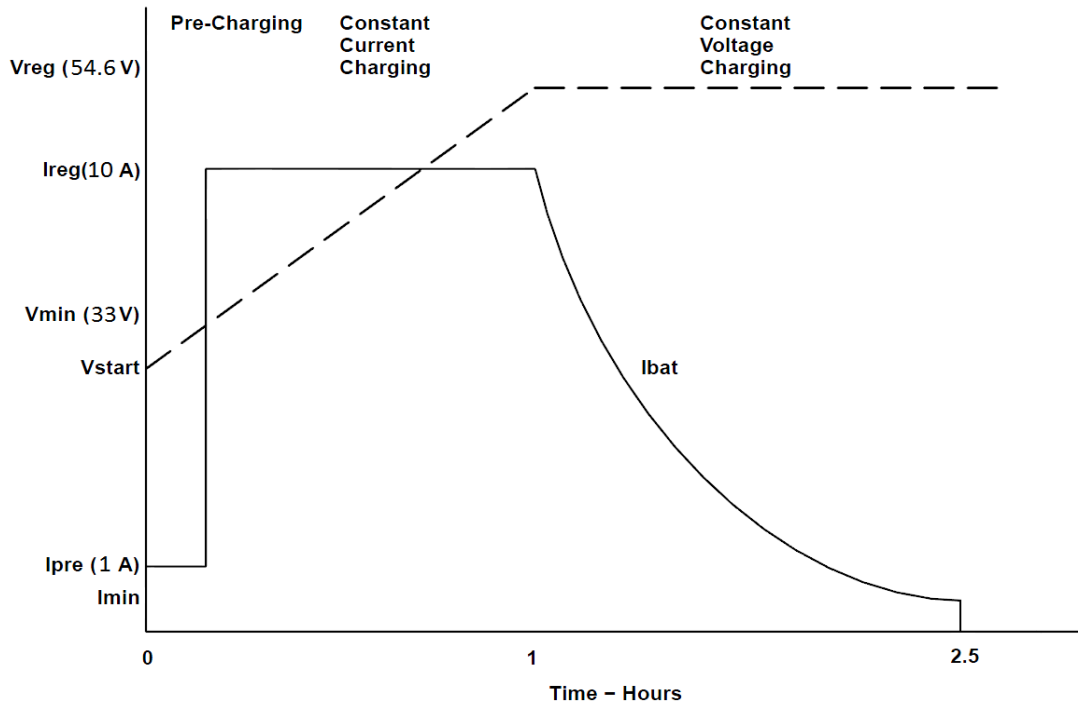


Figure 9: CC-CV voltage and current curves

2.3- The circuit

Lithium-Ion batteries are quite fragile and therefore require high-performance chargers. Their nature makes them very sensitive to undercharged voltages: if for instance the constant voltage stage undercharges the battery by 1.2%, there will be a capacity loss of 9%. Also, they cannot accept overcharge: when the battery operates between its operating voltages it works safely, but if the battery is forced to a higher voltage, some chemical reactions in the battery materials make it unstable and eventually causing a fire. In consequence, manufacturers of Li-

Ion batteries recommend using chargers of great accuracy. Otherwise, the life and reliability of the battery would get damaged every time it gets charged.

The purpose of this battery charger is to obtain power from a normal 120V and 60Hz USA wall outlet and supply the necessary voltage and current to charge the battery. In order to make this possible, the charger architecture is composed of several circuits. In this section, these circuits and their design calculations are introduced.

The following block diagram shows a schematic of the circuit and its components:

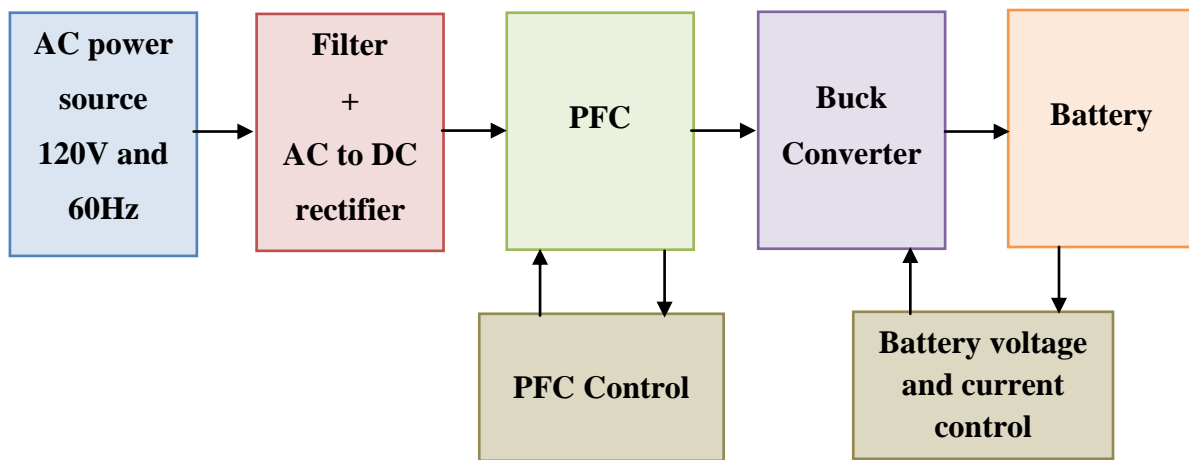


Figure 10: Block diagram with the sub-circuits of the battery charger

The six different elements composing the charger architecture are:

- AC power source: standard United States wall outlet.
- Full wave rectifier to turn the AC input into DC. This element also includes a simple filter.

- Power Factor Corrector (PFC): Boost converter controlled to raise the systems power factor near unity to comply with the standard regulations. It also delivers a high-level dc output voltage.
- Buck converter: to lower the PFC's output voltage to the value required for charging the battery.
- Battery: a model has been designed in PSIM to simulate the AllCell Li-Ion battery.
- Controls: both the PFC circuit and the Buck converter have fast and accurate controls to guarantee the desired values of current and voltage needed to charge the battery in a safe and efficient way.

Below is a more in depth description of the different elements that form this project.

2.3-1. The battery model

In order to design the model for the lithium ion battery, the AllCell datasheet was not sufficient. Therefore, more information was directly requested to the manufacturer, obtaining information about the actual electrical design of the battery (13 cells in series and 8 cells in parallel) and several charge and discharge curves for the model of the individual cell used in the battery under different conditions. The model has been designed for 25°C and a charging rate of approximately 0.5C.

Table 2 shows all the parameters requested for designing the lithium ion battery model in PSIM:

UNIVERSIDAD PONTIFICIA COMILLAS
 ESCUELA TÉCNICA SUPERIOR DE INGENIERÍA (ICAI)
 INGENIERO ELECTROMECAÁNICO

Symbol	Description	Value
N_s	Number of cells N_s in series in a battery pack	13
N_p	Number of cells N_p in parallel in a battery pack	8
E_{rated}	Rated voltage E_{rated} of the battery cell, in V	3.62V
E_{cut}	Battery voltage E_{cut} corresponding to the maximum capacity, in V	2.5V
Q_{rated}	Rated capacity Q_{rated} of the battery cell, in Ah	2.4Ah
$R_{battery}$	Internal resistance $R_{battery}$ of the battery cell, in Ohm	0.055 Ω
E_{full}	Full (or maximum) voltage E_{full} of the battery cell, in V	4.2V
E_{top}	Battery voltage E_{top} at the end of the exponential region in the discharge curve, in V	3.8V
E_{nom}	Battery voltage E_{nom} at the end of the nominal region in the discharge curve, in V	3.1V
Q_{max}	Maximum capacity Q_{max} of the battery cell, in Ah	2.9Ah
Q_{top}	Battery capacity Q_{top} at the end of the exponential region in the discharge curve, in Ah	0.2Ah
Q_{nom}	Battery capacity Q_{nom} at the end of the nominal region in the discharge curve, in Ah	2.4Ah
Initial State of Charge	Initial battery state of charge (SOC) (from 0 to 1)	X

Table 2: Parameters introduced in the Li-Ion battery model

The cell model used inside the AllCell battery is an LG 18650 MG1 (2.9Ah). These parameters refer to the individual cells inside the battery, being these values then multiplied by a factor (voltages multiplied by N_s , capacities multiplied N_p , and the resistance by N_s/N_p) to get the complete battery values.

Some of them were obtained directly from the cell datasheet (like E_{rated} , E_{cut} or Q_{rated}), but in order to get other parameters that refer more to the actual shape of the curves (E_{top} , Q_{top} , E_{nom} or Q_{nom}), the discharge curve was utilized.

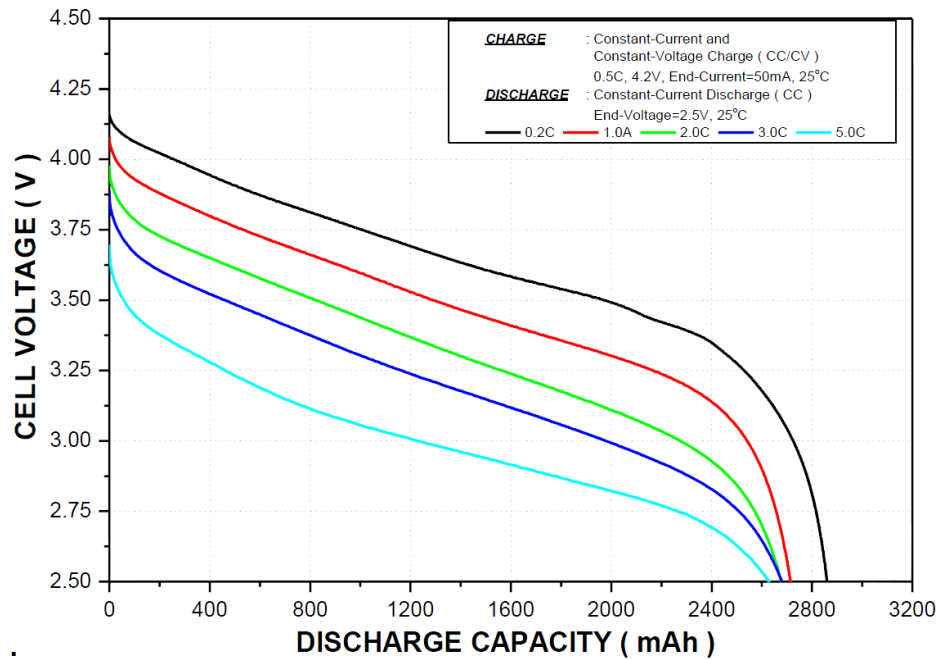


Figure 11: Discharge curves for the LG Li-Ion cell under different C-rates

Figure 11 shows the different discharge curves of the LG cell under different discharge rate conditions. The red curve shows the Voltage-Capacity curve when the battery cell is being discharged with 1A and it has been chosen to design the PSIM model. Making the assumption that the discharge curve of the whole battery will be analogous to the individual cell one, the circuit shown in Figure 12 has been used to simulate the discharge curve of the whole battery model.

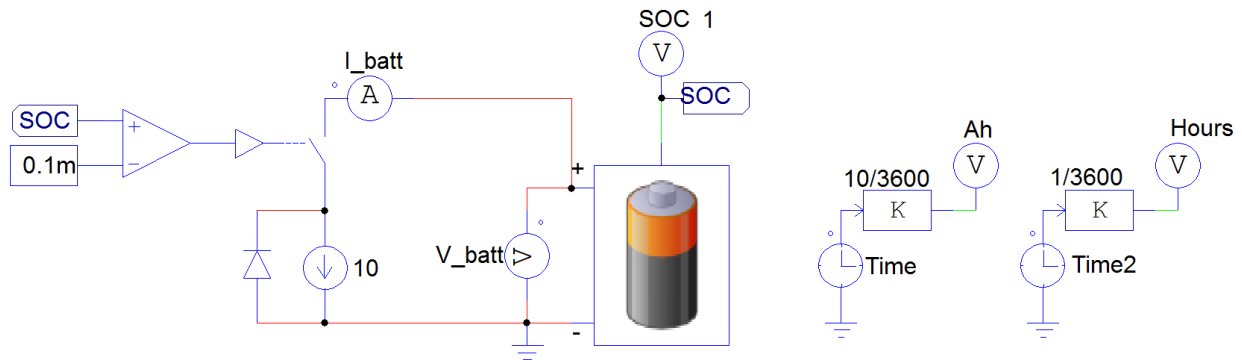


Figure 12: Simple discharge circuit

What this circuit does is discharge the battery at a current rate of 10A, starting at a SOC of 1, and stopping the discharge when SOC reaches 0.0001, measuring the voltage (V_{batt}) to obtain the curve. The simulation will be performed using two different X axis: Ah to obtain the Voltage-Capacity curve (which shows the total capacity the battery is able to provide when being discharged at 10A) and Hours, to see how much time it takes to discharge the battery with 10A.

After many trial-and-error iterations, the curve in Figure 13 was obtained.

From the curves, it can be observed that under these conditions (discharge with 10A) the battery has a maximum capacity of approximately 22Ah, a coherent value taking into account that according to the AllCell battery datasheet the nominal capacity is 20.8Ah. Also, it takes approximately 2.2 hours to discharge the battery at this rate.

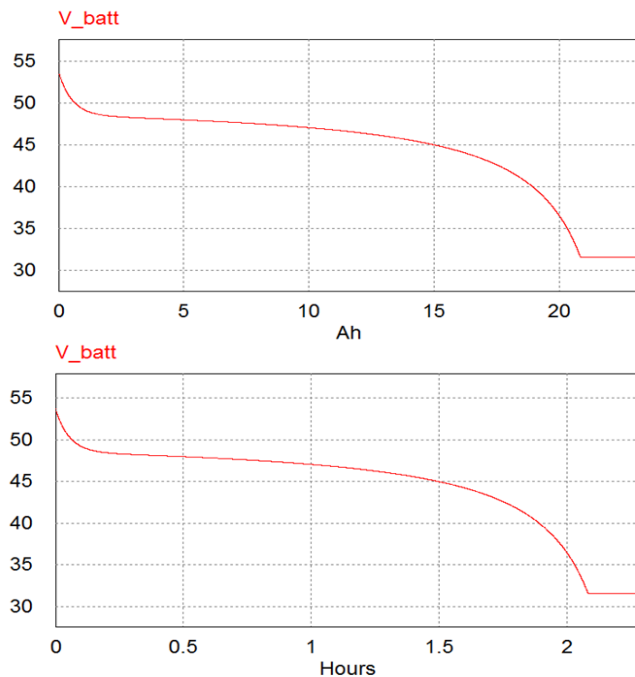


Figure 13: Battery model discharge curves

The model parameters were chosen to make the curve the most similar to the original one. It was impossible to achieve the steep and relatively constant slope of the original curve due to the simplicity of the model, but the resulting battery shows a very typical discharge curve. Therefore, this lithium-ion battery model was considered appropriate to begin the design of the charge circuit.

2.3-2. The AC power source

The first element used in the battery charger is the AC power source. This block simulates a standard wall outlet from the United States with $120V_{\text{rms}}$ and 60Hz. Although the element that simulates the power source in PSIM is ideal, a real wall outlet can have alterations in those values, with a voltage tolerance of plus 10% and minus 25% (i.e. $90V_{\text{rms}}$ to $132V_{\text{rms}}$) [6]. Since the battery must be charged at very specific voltage and current values, the charger's output must be independent of its input voltage. This control is performed in the next elements.

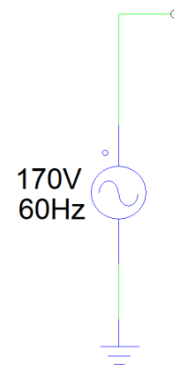


Figure 14: AC power source

2.3-3. The full wave rectifier

The Li-Ion battery must be charged using purely DC voltage and current, and therefore, the charger's output must be as smooth as possible. The first element inside the charger which starts converting the AC power supply voltage into DC is a diode bridge rectifier like the one shown in Figure 15. This full wave rectifier is composed by 4 individual diodes which conduct in pairs

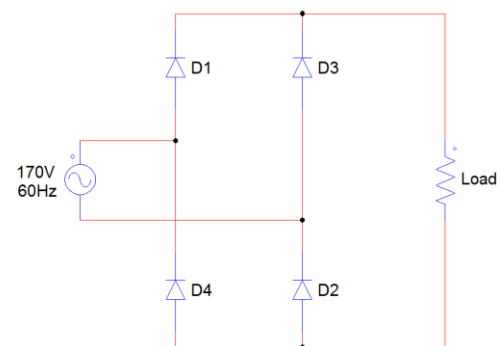


Figure 15: Bridge rectifier

in order to maintain the current always flowing in the same direction, even when the input voltage is negative.

During the positive half-cycle, diodes D3 and D4 will be reverse biased and therefore off. Only D1 and D2 will conduct, making the current flow in the direction shown in Figure 16. On the second half of the period, when the input voltage is in its negative half-cycle, the pairs of diodes will switch, being D1 and D2 off and D3 and D4 conducting. This way, the load current will keep flowing in the same direction, making the output voltage appear as the reversed input waveform.

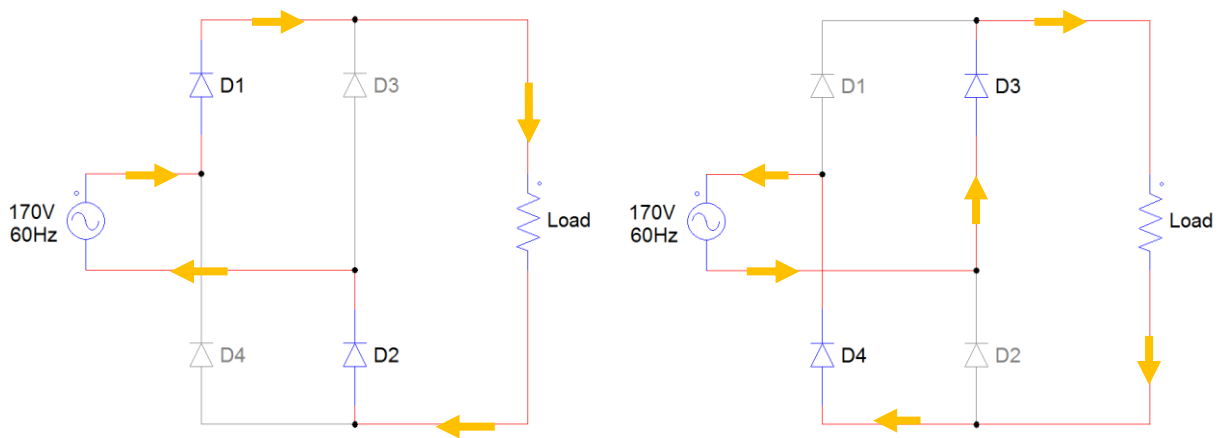


Figure 16: Bridge rectifier's modes of operation.

UNIVERSIDAD PONTIFICIA COMILLAS
ESCUELA TÉCNICA SUPERIOR DE INGENIERÍA (ICAI)
INGENIERO ELECTROMECAÁNICO

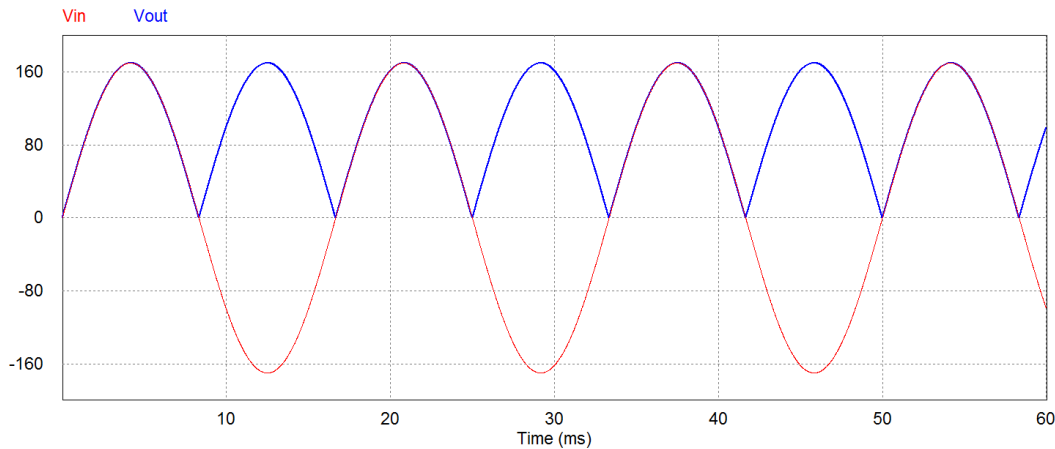


Figure 17: Bridge rectifier's input (red) and output (blue) voltage waveforms.

As a result, the output voltage will look like the blue waveform in Figure 17. The input voltage supplied by the wall outlet has $120V_{\text{rms}}$ and 60Hz , and a peak value of $\sqrt{2} \cdot 120V = 169.7V$. The rectifier's output (shown in Figure 17 as the blue waveform) will have twice the frequency, 120Hz , and a slightly smaller peak value, due to the fact that there will always be two diodes conducting with their respective voltage drops. The new peak value will be $169.7 - 2 * 0.7 = 168.3V$. This is not very important since, as it was mentioned before, the charger's output will not be affected by small perturbations in the input.

Nevertheless, the full wave rectifier's output is still not purely DC. Even if the frequency is higher and the average value is now different than zero, the ripple is still very high (roughly $170V$) and this is not desirable for this application. Some sort of filter must be applied to reduce this ripple as much as possible.

The first strategy used during the initial stage of the project was to use a passive filter: a capacitor in parallel at the rectifier's output to smooth the waveform. This capacitor converts the rectifiers output into an almost pure DC voltage by being charged to the peak value, and then slowly discharging until the next half-wave arrives. The bigger the capacitor the slower the

discharge and smaller the ripple will be. In order to calculate this smoothing capacitor the next calculations were made:

First, the load was calculated. This value was calculated in an extreme condition where the load would be consuming 1000W (the AllCell battery has a rated power of 1000W, but this value will never be achieved during the charging process since it is being charged at roughly 0.5C). With $V_m = 170V$ and $P = 1000W$:

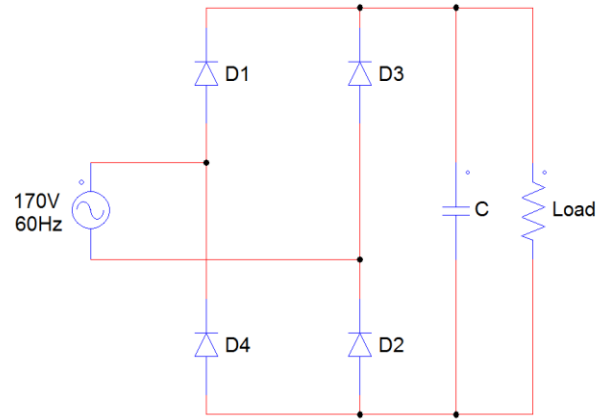


Figure 18: Bridge rectifier with smoothing capacitor

$$R_{Load} = \frac{V_m^2}{P} = \frac{170^2}{1000} = 28.9\Omega$$

Now, the following formula [7] was used to calculate an appropriate value for the capacitor, taking into account that we want a ripple of 1%, ($\Delta V_m/V_m = 0.01$):

$$\Delta V_m \approx \frac{V_m}{2fRC} \rightarrow C = \frac{1}{2fR \frac{\Delta V_m}{V_m}} = \frac{1}{2 \cdot 60 \cdot 28.9 \cdot 0.01} = 28.8mF$$

As a result, the simulation for the full wave rectifier with parallel capacitor (Figure 18) is shown in Figure 19. The output waveform is now a far purer DC.

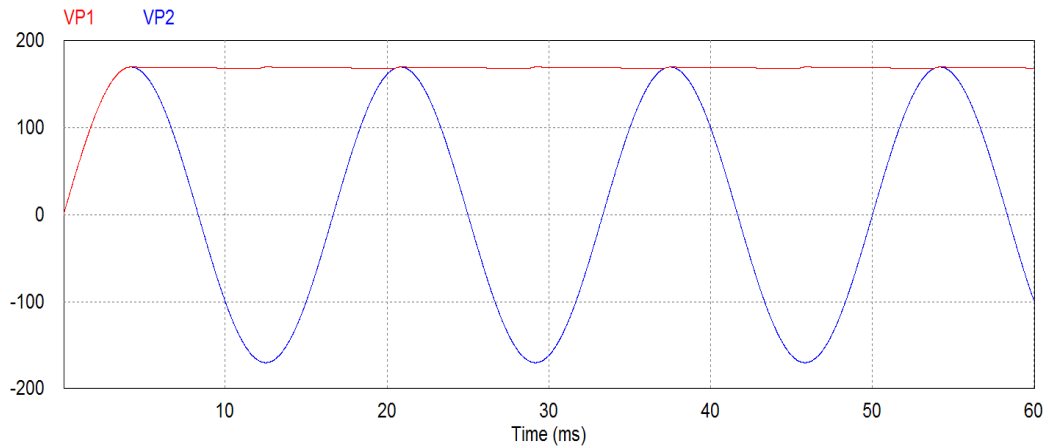


Figure 19: Bridge rectifier's input (red) and output (blue) voltage waveforms with the smoothing capacitor.

2.3-3.1. Drawbacks of this rectifier

The advantage of this type of ac-dc rectifier is that with a very simple topology it delivers a decent dc output with very little ripple, as it is shown in Figure 19.

Nevertheless, the strategy of using a smoothing capacitor to obtain a purer dc output voltage has two main disadvantages:

- As it was mentioned before, in order to minimize the voltage ripple, the smoothing capacitor must have a very high value (in this case roughly 30mF). These types of capacitors are expensive and very large, making them undesirable for the designed circuit.
- Another important drawback of using a passive filter to smooth the output waveform into a purer dc voltage is that the overall device has very inefficient power consumption, i.e. it has a low power factor. This can be seen when simulating the input voltage and current of the topology shown in Figure 20.

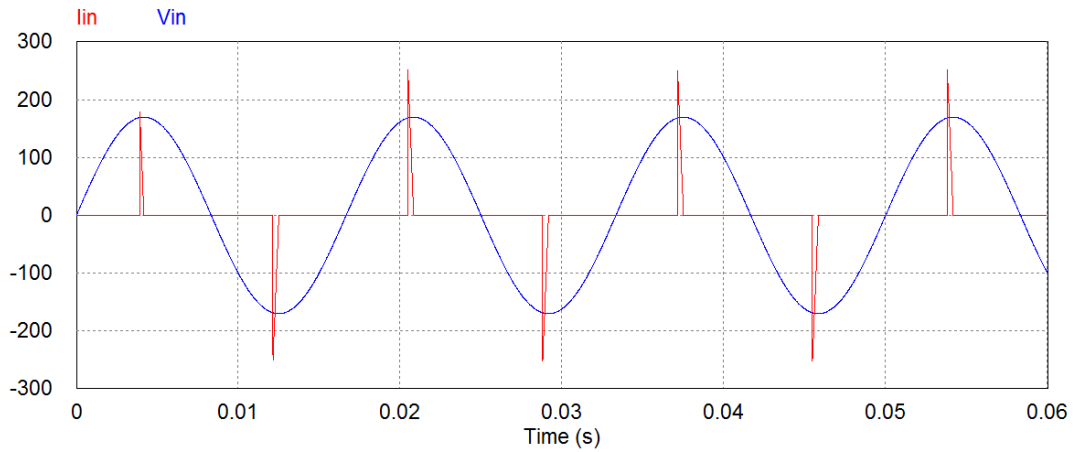


Figure 20: Input voltage (blue) and current (waveforms).

It shows the input voltage and current. This topology has a power factor of 0.25, which means that three fourths of the input power are wasted. This is completely unacceptable in any electronic device, so a different strategy will have to be followed in order to obtain the desired dc voltage, as well as incrementing the power factor.

The chosen solution has been to remove the smoothing capacitor and use a power factor corrector (PFC) instead.

2.3-4. Power factor correction (PFC)

When designing an electronic device, and especially in the case of battery chargers (where the whole purpose is to transmit power), power efficiency is a major objective. This power efficiency is expressed with the power factor, or PF, which measures the ratio between the real power P (the one used by the load) and the input power (or apparent power S). It represents the phase lag between voltage and current, ranging from 0 to 1, where 1 represents 100% of the input power is being used and both waves are in phase.

UNIVERSIDAD PONTIFICIA COMILLAS
ESCUELA TÉCNICA SUPERIOR DE INGENIERÍA (ICAI)
INGENIERO ELECTROMECAÁNICO

In non-linear systems, time lags, distortion and harmonics are introduced causing a more inefficient use of the energy drawn from the power source, and this is clearly shown in the form of the input current. In an ideal situation, this current should follow the input voltage in a synchronized way, just as if the load was a pure resistor, without introducing any current harmonics. In the full wave rectifier with the parallel capacitor, the input current was extremely distorted, showing sharp spikes instead of a smooth sinusoidal curve.

In the industry, power factor requirements used to affect only to manufacturers of inductive motors. Big penalties were applied to the companies that did not comply with the regulations, in an effort to stimulate improvements in their power consumption. However, not many years ago, these power regulations were also expanded to lower-power supplies, affecting consumer electronics. In 2001, the European Union put EN61000-3-2 [8], establishing the limits in terms of harmonics that the different types of devices were allowed to have. For some devices considered Class A (household appliances, audio equipment, etc) the regulations allow them to have a PF of around 0.9. On the other side of the spectrum, Class D devices (personal computers, tablets, laptops, etc) have much more stringent regulations, being obliged to have a PF=1. This charger has been considered to be among Class D devices, and therefore the power factor will have to be very high.

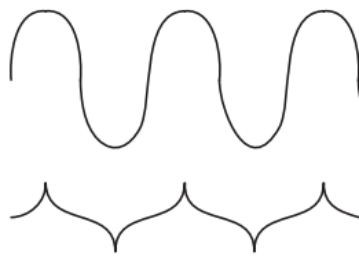


Figure 22: Class A voltage and admissible current waveform.

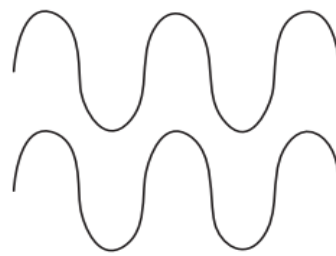


Figure 21: Class D voltage and required current waveform.

With the purpose of not only delivering a dc voltage at its output, but mainly to increase the power factor of the system, a power factor corrector (PFC) has been implemented between the full wave rectifier and the Buck converter. The chosen topology to implement the PFC has

been a CCM boost converter. This is because the input voltage may vary and a step up converter is more convenient (eliminating the buck converter for being a step down converter and the buck-boost for having a high switch voltage stress). Also, in order to control the PFC, the input current to the converter will be measured, and since the inductor in the boost converter is in the input side, it guarantees a smooth input current waveform which is much easier to filter and measure.

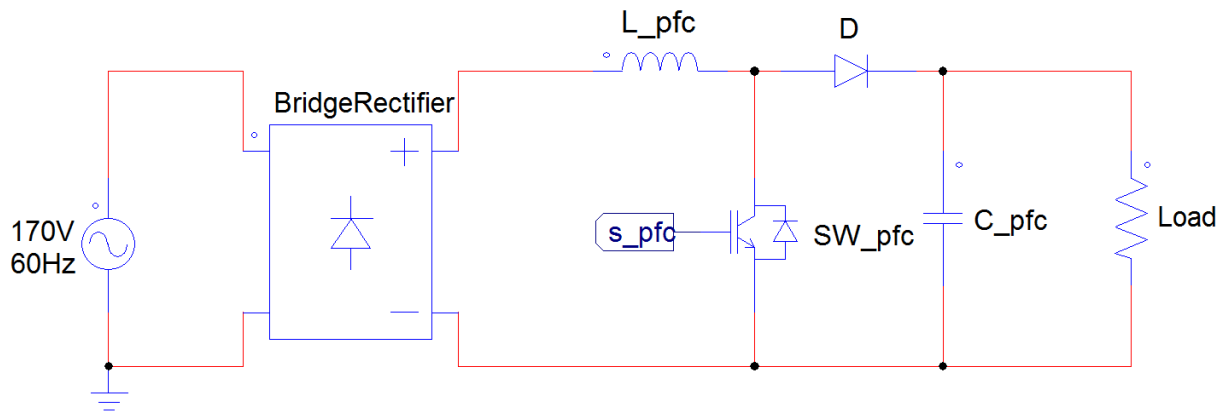


Figure 23: Topology for both the bridge rectifier and the PFC.

2.3-4.1. Design considerations

Figure 23 shows both the full wave rectifier (the 4 diodes have been substituted by a block with the same function, for visual simplicity of the circuit) and the boost converter. The latter has been designed with the following specifications:

- The PFC boost converter can operate in discontinuous conduction mode (DCM), critical conduction mode (CrCM) and continuous conduction mode (CCM). The latter was chosen due to the fact that the peak current is lower than with the other two modes, the turn-off losses in the switch are lowest and the HF ripple current is the lower in amplitude. Nevertheless, the turn-on losses will be bigger than in CrCM, and an ultra-fast recovery diode will be needed to compensate this effect.

UNIVERSIDAD PONTIFICIA COMILLAS
 ESCUELA TÉCNICA SUPERIOR DE INGENIERÍA (ICAI)
 INGENIERO ELECTROMECAÁNICO

- The design will be done for the following specifications:

Parameter	Value
Input voltage	90-132V _{AC} 60Hz
Output voltage	200V
Maximum power	1000W
Switching frequency	40kHz
Inductor current ripple	25%
Output voltage 120Hz ripple	10V _{p-p}
Hold-up time (time it takes to the output voltage to go below regulation if the AC input voltage is removed [10])	16.6ms at V _{o,min} =150V

Table 3: Specifications for the PFC design.

2.3-4.2. Design of the components

First, the filter inductor will be designed [9]:

$$L = \frac{1}{\%Ripple} \cdot \frac{V_{ac,min}^2}{P_o} \left(1 - \frac{\sqrt{2} \cdot V_{ac,min}}{V_o} \right) \cdot T =$$

$$= \frac{1}{0.25} \cdot \frac{90^2}{1000} \left(1 - \frac{\sqrt{2} \cdot 90}{200}\right) \cdot \frac{1}{40 \cdot 10^3} = 0.3mH$$

The maximum current flowing through this inductor (which will be useful when choosing the real component) is:

$$I_{L,max} = \frac{\sqrt{2} \cdot P_o}{V_{ac,min}} \cdot \left(1 + \frac{\%Ripple}{2}\right) = \frac{\sqrt{2} \cdot 1000}{90} \cdot \left(1 + \frac{0.25}{2}\right) = 17.67A$$

Now, the output capacitor will be designed to meet the specifications (hold-up time of 16.6ms and 10V output voltage ripple). Two calculations will be made (on for each requirement), and the one with the largest result will be chosen:

$$C_o \geq \frac{2 \cdot P_o \cdot t_{hold}}{V_o^2 - V_{o,min}^2} = \frac{2 \cdot 1000 \cdot 16.6 \cdot 10^{-3}}{200^2 - 150^2} = 1.8mF$$

$$C_o \geq \frac{P_o}{2\pi \cdot f_{line} \cdot \Delta V_o \cdot V_o} = \frac{1000}{2\pi * 60 * 10 * 200} = 1.33mF$$

As a result, and in order to comply with all the requirements, the capacitor has been chosen with a value of C=1.8mF.

2.3-4.3. Controlling the PFC

In order to control the PFC boost converter, a double loop control method is used [13]. There is a cascaded control with an inner current loop and an outer voltage loop. This will allow the converter to not only increase the power factor until almost reaching 1, but also delivering a

dc output that will be the voltage level that the buck converter will regulate. Figure 24 shows a diagram of the whole closed loop system.

First, the inner current loop measures the current in the boost converter's inductor and makes the input current's profile follow a sinusoidal waveform. This control loop is designed to be much faster than the outer voltage loop, so that the inductor current can change much faster than the output voltage. The bigger the difference in the dynamics speeds between both loops, the easier it will be to design them, since they won't interfere with each other.

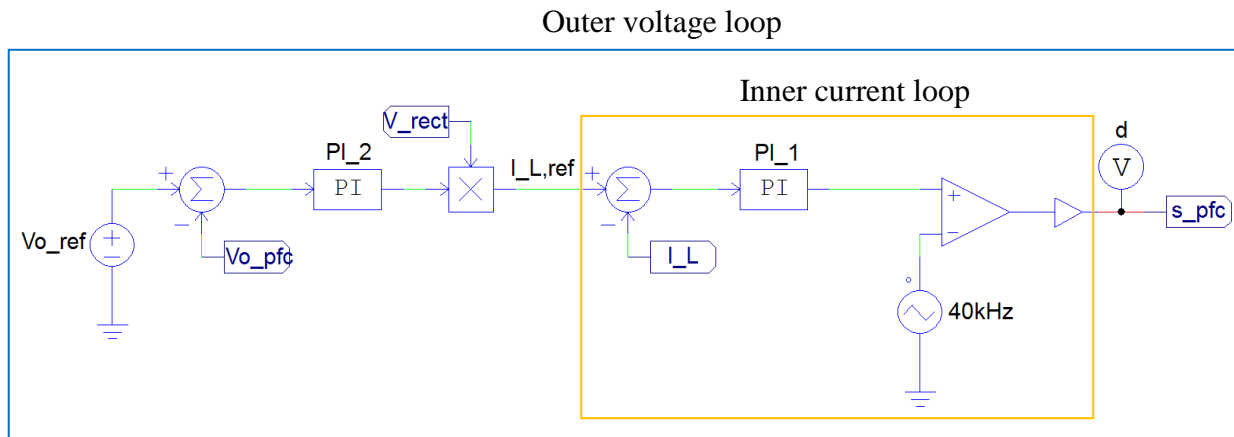


Figure 24: PFC inner and outer control loops.

As it is shown in Figure 24, the inner current loop receives the current reference $i_{L,ref}(s)$ (generated by the outer voltage loop) and it is compared with the actual inductor current $i_L(s)$ measured at the input of the PFC. Then a PI controller is introduced to eliminate the steady state error and amplify the low frequency gain. The values chosen for the PI controller are gain $K = 0.4$ and time constant $T = 0.84\mu s$. Notice how fast this control is. This is because in order to follow the current sinusoidal reference, the switch's duty cycle will be controlled to charge and discharge the inductor really fast in a way so that the average value of this current is equal to the reference. This way, the current will follow the input voltage in a synchronized fashion, which will make the power factor increase until almost reaching 1. After the PI controller, the

signal goes to the non-inverting input of a comparator, where it is compared with a 40kHz sawtooth carrier waveform. This way, the duty cycle signal is generated and sent to the switch.

Now, the output voltage loop is the one that by measuring the PFC's input voltage, generates the inductor current reference to be followed in the inner current loop. First, a voltage reference was set in $V_{o,ref} = 6V$. This is because the desired PFC's output voltage is 200V, and the voltage sensor has a gain of $G = 0.03$, therefore $V_{o,ref} = 200 \cdot 0.03 = 6V$. Then, this reference is compared with the actual measure of the output voltage and this error signal is sent to a PI controller. This PI controller has the same objective (increase the low frequency gain) and the chosen values are gain $K = 1$ and time constant $T = 0.03$, which shows that this loop is much slower. This signal is then multiplied by the rectifier's output voltage, generating an inductor current reference $I_{L,ref}$ that is sinusoidal and synchronized with the charger's input voltage. This reference is then the input to the inner current loop.

2.3-5. The buck converter

After the AC input has been converted to DC, the voltage and current values must be controlled in order to perform the Constant Current – Constant Voltage charging method. This is achieved using a step-down DC-DC converter, which converts an input DC voltage into a lower DC output voltage.

The simplest topologies are the basic linear regulator and the basic switching converter, both composed of a single transistor. The basic linear regulator uses the transistor in its linear zone, operating like a variable resistance. By controlling the base current of the transistor, the output voltage can be adjusted from 0 to the input voltage. The problem with this topology is the low efficiency, since a lot of power is lost in the transistor, making this converter unsuitable for this application.

UNIVERSIDAD PONTIFICIA COMILLAS
ESCUELA TÉCNICA SUPERIOR DE INGENIERÍA (ICAI)
INGENIERO ELECTROMECAÁNICO

The second simplest is the basic switching converter. It is a more efficient alternative since the transistor is either completely on or completely off (saturation or cutoff regions). By controlling the time the switch is closed (controlling the duty cycle), the average output voltage can be controlled. But this topology does not deliver a purely DC voltage as an output, something necessary for charging a battery, making this topology unsuitable for this application too.

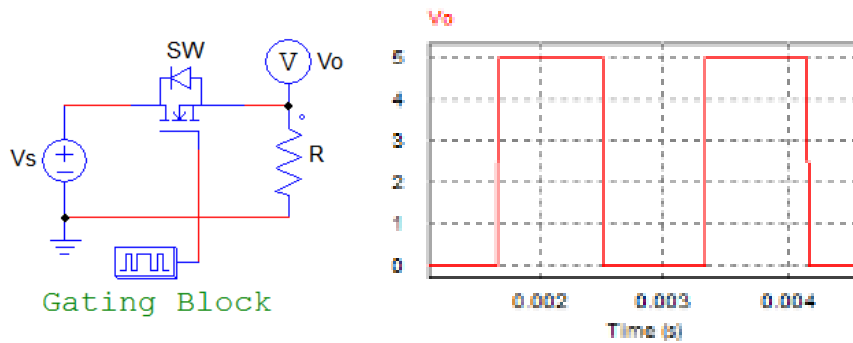


Figure 25: Basic switching converter and its output voltage.

This brings us to the Buck converter. As opposed to a simple step-down converter, the Buck converter produces a purely DC output by adding an LC low-pass filter after the switch. Also, a diode is added to provide a path for the inductor to discharge its current whenever the switch is open. Figure 26 shows the topology and its equivalent in both modes. In mode 1 (b), the switch is closed and the diode is reverse-biased. The output current will linearly increase as the inductor gets charged. Then, in mode 2 (c), the switch is open and the diode is conducting. Now the output current will linearly decrease as the inductor discharges through the diode.

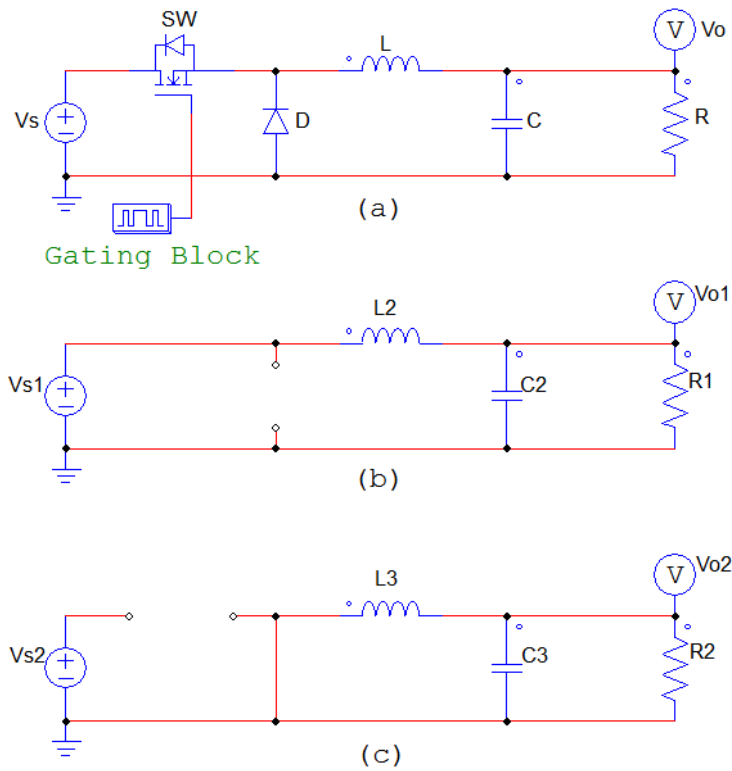


Figure 26: (a) Buck dc-dc converter; (b) Equivalent circuit for the switch closed; (c) Equivalent circuit for the switch open.

2.3-5.1. Design considerations

- The designed buck converter operates in continuous-current mode (CCM), which means that the inductor never fully discharges when the switch is off.
- The switch will be controlled with a fixed frequency of $40kHz$. This frequency was decided taking into account two important factors: two important design considerations are keeping the components (inductor and capacitor) small and maximizing the

efficiency. These are directly affected by the choice of the switching frequency: low values of frequency (above $20kHz$ to avoid audio noise) will entail bigger components. The minimum inductor value for maintaining CCM is inversely proportional to the switching frequency. On the other hand, if what matters most is the size of and it is decided to increment the frequency ($500kHz$ is the preferred value by many designers but it can go higher than $1MHz$), the tradeoff will be a decreased efficiency, since there will be a bigger power loss in the switch.

For this specific design, efficiency was considered more important than the components size, choosing a switching frequency of $40kHz$.

- Finally, since the objective of this buck converter is to first keep a constant output current and then a constant voltage, an control system will be designed (and explained after the components' design) with this purpose.

2.3-5.2. Design of the components

During the charging process, the battery voltage ranges from $40V$ to $54.6V$. That is equivalent to the output voltage in the Buck converter so the duty ratio for continuous-current operation is:

$$D = \frac{V_o}{V_s} \rightarrow \frac{40}{200} \leq D \leq \frac{54.6}{2} \rightarrow 0.2 \leq D \leq 0.273$$

For the design of the components the duty ratio $D=0.2$ has been used in order to guarantee continuous-current operation (CCM).

The first and most important parameter to be determined is the inductor's value. It will be critical to guarantee CCM and it will also decide the output current's ripple.

As it was aforementioned, the chosen switching frequency is $40kHz$. Also, the R used in the functions is the one that was calculated when designing the full wave rectifier: $R=28.9\Omega$.

The minimum inductor size is:

UNIVERSIDAD PONTIFICIA COMILLAS
 ESCUELA TÉCNICA SUPERIOR DE INGENIERÍA (ICAI)
 INGENIERO ELECTROMECAÁNICO

$$L_{min} = \frac{(1 - D)R}{2f} = \frac{(1 - 0.2) * 28.9}{2 * 40 * 10^3} = 289\mu H$$

To guarantee continuous-current operation, at least a 25% bigger inductor should be used:

$$L = 1.25 * L_{min} = 1.25 * 289 \approx 361\mu H$$

The average inductor current during the constant current stage is $I_L = 10A$ (maximum charge current specified for this battery). The most important factor when selecting a value for the inductor is the current ripple. Since the battery must be charged in DC, the ripple must be as small as possible. A ripple value of $\Delta i_L = 1A$ was chosen, being a 10% of the current value. The ripple will change as the output voltage increases, so the inductor was calculated for both scenarios ($V_o = 40V$ and $V_o = 54.6V$) and then an intermediate value was chosen:

$$\Delta i_L = \left(\frac{V_s - V_o}{L} \right) \cdot DT$$

$$L_{40V} = \frac{(V_s - V_o)}{\Delta i_L} \cdot DT = \frac{(200 - 40)}{1} \cdot 0.2 * \frac{1}{40 \cdot 10^3} = 0.8mF$$

$$L_{54.6V} = \frac{(200 - 54.6)}{1} \cdot 0.273 * \frac{1}{40 \cdot 10^3} = 0.99mF$$

As a result, the chosen inductor has a value of $L = 0.9mF$.

Secondly, the capacitor value is selected to guarantee an output voltage ripple ($\Delta V_o/V_o$) smaller than 1%. A big output voltage ripple can be caused by an insufficient capacitance or by a big equivalent-series resistance (ESR) in the capacitor. Therefore, it is desirable to select a big capacitance with a low ESR. It has been designed when $D=0.273$, to guarantee a small ripple during the whole charging process.

$$C = \frac{1 - D}{8L(\Delta V_o/V_o)f^2} = \frac{1 - 0.273}{8 * 0.9 * 10^{-3} * (0.01) * (40 * 10^3)^2} = 6.31\mu F$$

UNIVERSIDAD PONTIFICIA COMILLAS
 ESCUELA TÉCNICA SUPERIOR DE INGENIERÍA (ICAI)
 INGENIERO ELECTROMECAÁNICO

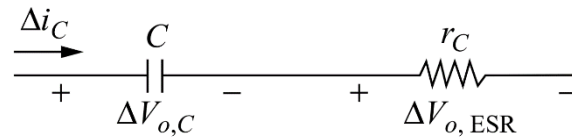
This value was then rounded to $C = 6.5\mu F$ to facilitate the component search.

Now that the values of C and L are chosen, the cut-off frequency of the LC filter can be calculated as:

$$f_c = \frac{1}{2\pi\sqrt{LC}} = \frac{1}{2\pi\sqrt{0.9 \cdot 10^{-3} \cdot 6.5 \cdot 10^{-6}}} \approx 2kHz$$

This frequency is much lower than the switching frequency chosen to open and close the converter's switch. The effect of this is that the LC filter won't be able to see the rapid changes in the switch, and this will guarantee a cleaner DC output.

Furthermore, to make the design more realistic, a real capacitor has been designed. That means that its equivalent series resistance (ESR) has been taken into account. The ESR may have a significant effect on the output voltage ripple, and without being considered the experimental voltage ripple value could be greater than the theoretical. The resultant model of the capacitor is:



$$\frac{\Delta V_o}{V_o} = 0.01 \quad \rightarrow \quad \Delta V_o = 0.01 * 54.6V = 546mV$$

The voltage ripple of the real model of the capacitor can be approximated to the voltage variation produced by the equivalent series resistance only:

$$\Delta V_o = \Delta V_{o,C} + \Delta V_{o,ESR} \approx \Delta V_{o,ESR} = r_C \Delta i_C = r_C \Delta i_L$$

$$r_C = \frac{\Delta V_o}{\Delta i_L} = \frac{546mV}{1A} = 546m\Omega$$

This value is only theoretical. Nowadays, capacitors are designed with lower ESR values, as it will be shown later on in the component selection chapter.

2.3-5.3. Controlling the buck converter

This buck converter must have a control system that allows the system to perform the constant current constant voltage method automatically and with great accuracy. In the first stage of the charging process, the buck converter will be controlled to keep a constant current of 10A at its output. The voltage will then slowly increase until it reaches 54.6V. At that moment, the current control will switch to a voltage control to maintain a constant voltage of 54.6V. Then the uncontrolled current will rapidly decrease and when it drops to a value of 1A, another control will finish the charging process by opening the buck converter's switch (i.e. disconnecting the battery from the voltage source). Figure 27 shows a flowchart diagram of this process.

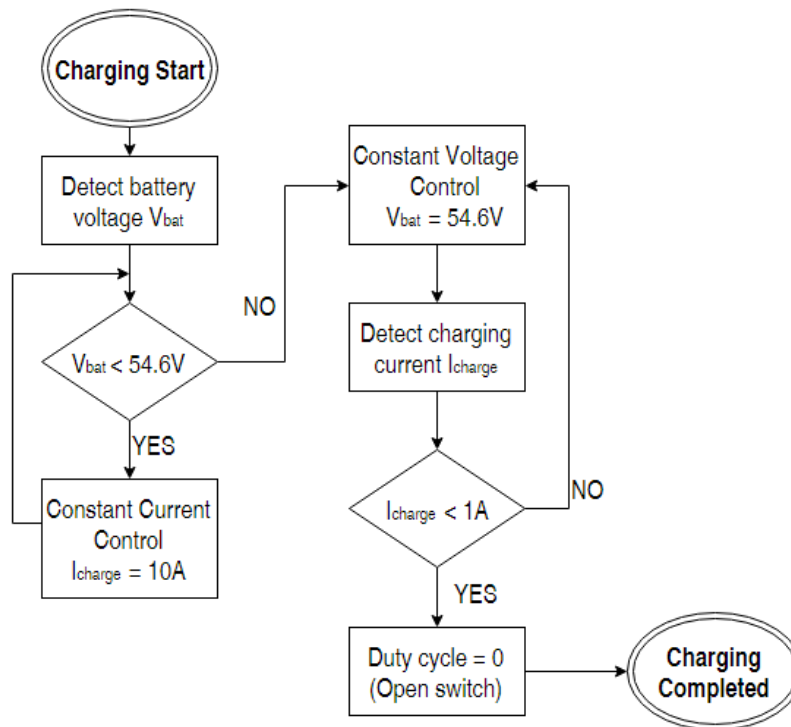


Figure 27: Flowchart diagram of the CC-CV process executed by the buck converter's controls.

Below is a more in depth explanation of these control systems. The current and voltage controls are analogous so the detailed explanation of the feedback loop will only be done for the voltage control. Then a short description of the current control will be done. Finally, the control systems that make it possible to change from on type of control to another will be explained in detail.

a) Voltage control

Normally, dc-dc converters like the one being designed are meant to have a constant output voltage that stays unaltered in case of disturbances in the input, load or circuit elements. This would be impossible just by setting a constant duty cycle to control the converters switch. This is because the duty cycle, calculated as $D = V_o/V_{in}$ is relative to the input voltage. Therefore, if there is a disturbance in the input and the duty cycle is constant, the output voltage will follow the disturbance. In this system this is unacceptable since, as it was mentioned earlier, Li-Ion batteries should never be charged with higher voltages than its rated maximum since this would cause a lot of stress in the battery and probably damaging it.

Instead, dc-dc converters use negative feedback to regulate and automatically adjust their output voltage, forcing it to follow a reference value in steady state but also in case of disturbances in the input or in the output load. This way, the designer guarantees that the charger will be very accurate and it won't damage the battery by causing it undesired stresses. Figure 28 shows the buck topology and the way this control is implemented.

The way this control system works is, firstly, the output voltage $v(t)$ is measured (usually with a voltage divider using precision resistors). This sensor may or it may not have a gain $H(s)$. In this case its value is $H(s) = 1$.

Then this measured value is compared with the reference voltage value v_{ref} , obtaining the error signal $v_e(t)$. Ideally, this error signal would be zero, but in reality it is always different than 0. However, if the control loop is well designed, this error signal will be small and its steady state error will be 0.

The next step is to use a compensator $G_c(t)$ to amplify the error signal, obtaining the control voltage $v_c(t)$. The objective of this control loop is to guarantee that the output voltage stays stable in the value specified by the reference. Therefore, the compensator used for this control loop is a PI controller, since it increases the low-frequency loop gain. This improves the rejection of low-frequency disturbances and guarantees a zero steady-state error.

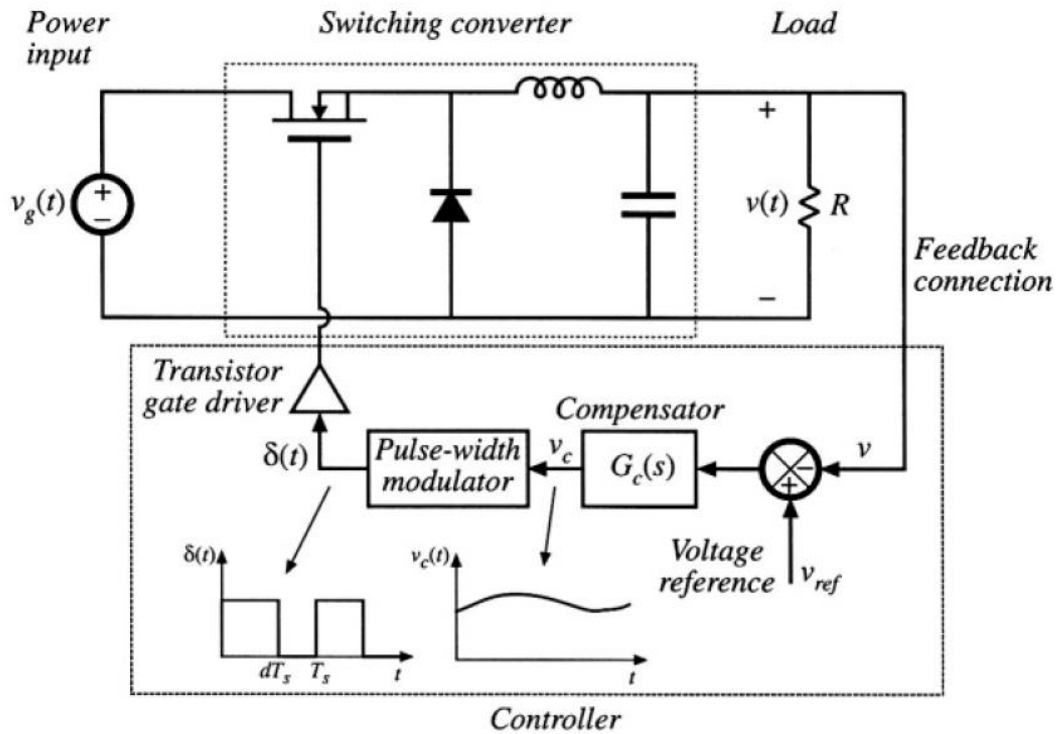


Figure 28: Buck converter topology with feedback loop.

In order to design the compensator, the converter model must be found. A buck converter is a switching circuit and it therefore has two modes: when the switch is closed it is in charging status, and when it is open it is in discharging status. Hence, the system has two different topologies, making it a nonlinear system. In order to get the transfer function needed to design the control, the averaged small-signal converter model for CCM must be calculated. Since the only nonlinear part of the topology is caused by the switching components (transistor and diode), if the average of the switching waveforms over a single period is calculated, then a linear model

can be derived and substituted in the original topology. This way, a linear model can be approximated in order to obtain the transfer function.

After many calculations [11] the resulting line-to-output transfer function for the buck converter defined as:

$$F(s) = \frac{D}{1 + \frac{L}{R}s + LCs^2} = \frac{0.273}{1 + \frac{0.9 \cdot 10^{-3}}{28.9}s + 0.9 \cdot 10^{-3} \cdot 6.5 \cdot 10^{-6}s^2}$$

$$= \frac{0.273}{5.85 \cdot 10^{-9}s^2 + 3.114 \cdot 10^{-5}s + 1}$$

This model was designed using an ideal version of the buck converter, i.e. without taking into account the series resistors that come with the inductor and capacitor. Therefore, the resulting values for the PI controller won't be definitive, but an approximated value that will serve as a starting point in case the controls must be varied once the real components are introduced and the whole circuit is integrated.

The PI controller has the following transfer function:

$$C(s) = K \frac{1 + Ts}{Ts}$$

The objective system will have zero error when following the reference, and it will be overdamped in order to avoid the output voltage to go over the desired voltage reference (if the output voltage goes above 54.6V it could damage the Li-Ion battery). Therefore, the following values for K and T were chosen:

$$K = 2 \quad T = 0.001$$

In order to analyze the resulting system, the closed loop transfer function G(s) is simulated next to the line-to-output transfer function in the frequency domain (Nichols Chart) and in the step response.

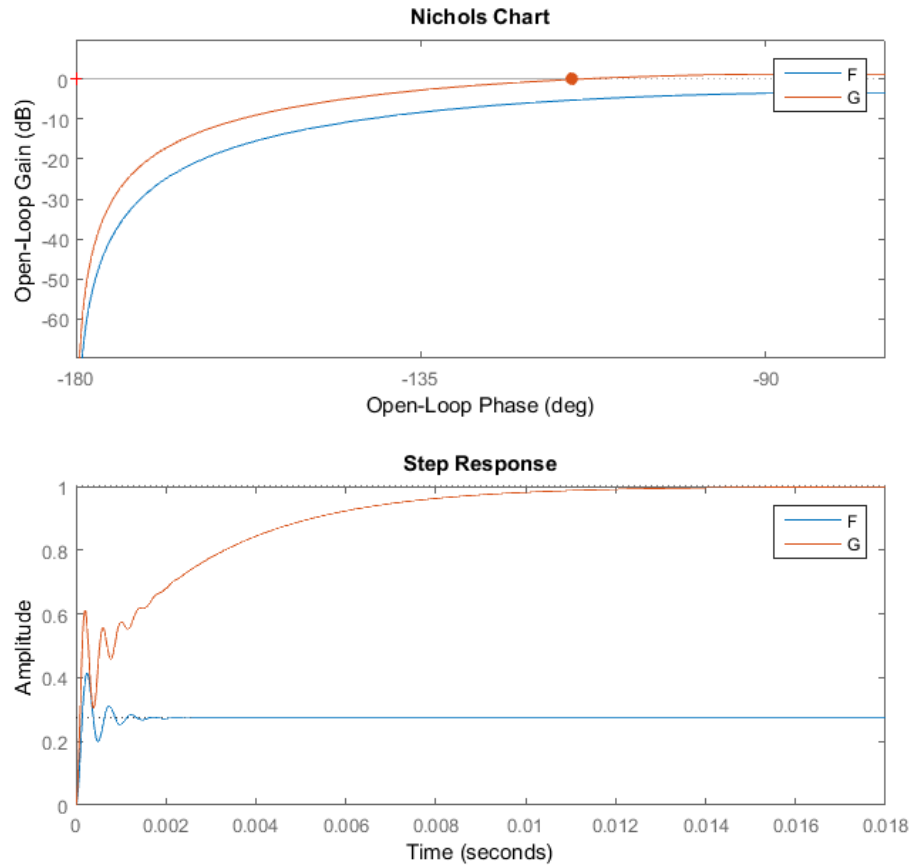


Figure 29: Nichols chart and step response of the resulting controlled system.

With this values, as it can be observed in Figure 29, the resulting system is overdamped (in the step response it can be seen how the response never goes above 1, and the settling time is equal to 0.01s), and how there is no steady state error when following the reference.

Finally, a pulse-width modulator (PWM) will be used to generate a logic signal $\delta(t)$ that controls the converter's switch to turn on or off. The objective of the PWM is to generate a duty cycle $d(t)$ proportional to the control voltage, so that if the control voltage increases, the duty cycle will increase as well. This is achieved by using a comparator whose noninverting input will receive the control voltage, and it will be compared with a sawtooth waveform (with amplitude 1 and frequency 40kHz). The output of the comparator will be the duty cycle signal $\delta(t)$ that controls the converter's switch. The frequency with which the switch will open and close is

40kHz (the one used when designing the buck's components). Figure 30 shows the diagram for the PWM modulator.

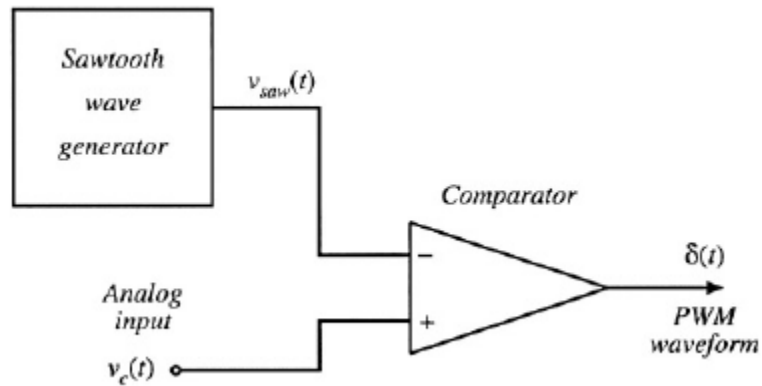


Figure 30: Diagram for the PWM modulator.

Finally, Figure 31 shows circuit that was implemented in PSIM to control the voltage. Notice how the reference value is set on $V_{ref} = 54.6V$.

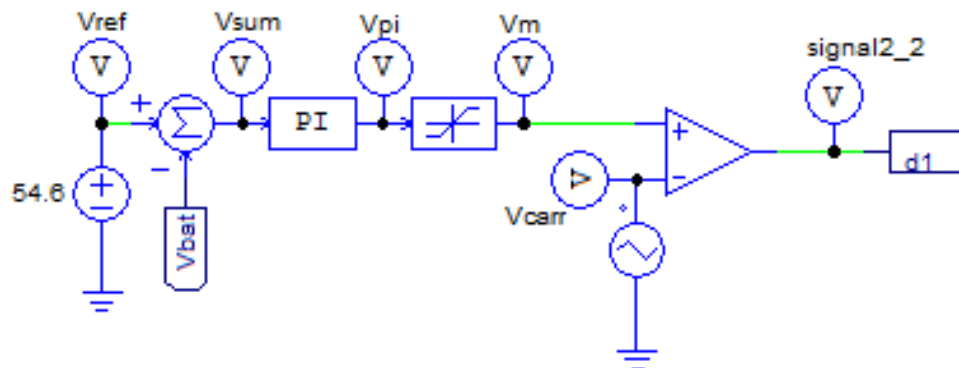


Figure 31: Buck converter's voltage control circuit implemented in PSIM.

As a result, if for instance a disturbance in the input makes the input voltage increase, the output voltage will try to increase too, but the control system will detect this and lower the value of the duty cycle so the switch is open for longer and the charging status (mode 1) becomes shorter.

b) Current control

As it was aforementioned, the current control is analogous to the voltage one. Figure 32 shows the designed circuit for this control. The reference is set in $I_{ref} = 10A$ and the PI parameters are $K=0.35$ and $I=0.001$.

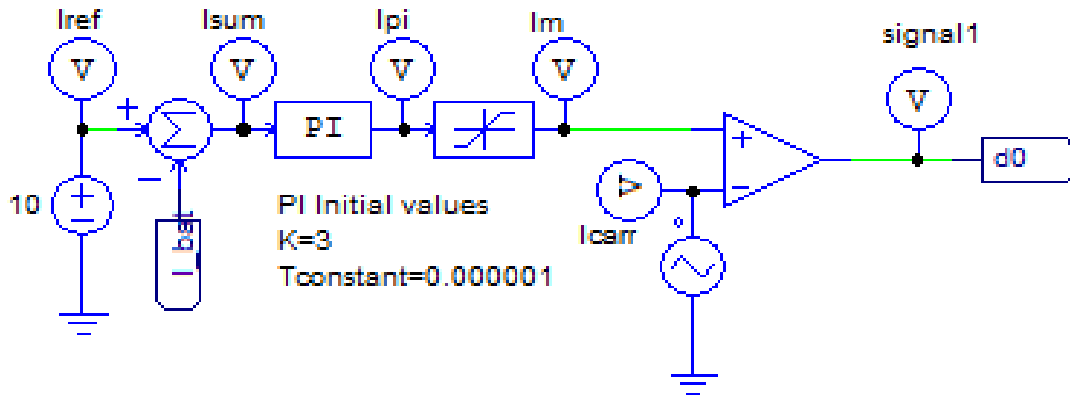


Figure 32: Buck converter's voltage control circuit implemented in PSIM.

c) Other controls.

The charging process requires two stages: constant current, constant voltage. The controls for each stage are already explained, but there are a few controls that decide which of the controls must send the duty cycle signal at a time. A multiplexor will receive the three signals (constant current control, constant voltage control and duty cycle=0 for when the process is finished), and will send only one at a time. To decide which duty cycle signal must be sent, two comparator circuits will measure voltage and current to determine the ongoing charging stage. Below, each circuit is explained.

First, a comparator measures the output voltage, and whenever the 54.6V limit is reached, it sends a signal s_0 to the multiplexor to change from the constant current control to the constant voltage control. The initial circuit was a simple comparator, and it would have worked correctly if the measured voltage was perfect DC. But the real output voltage has a small ripple, and this caused a big problem when the 54.6V limit was reached. Since the voltage waveform is sinusoidal, the voltage limit was not crossed once, but many consecutive times with a frequency of 40kHz. This caused the multiplexor to change from CC to CV many times with a very fast frequency, and this is unacceptable. Figure 33 shows how although the 54.6V limit has been reached, the control signal does not permanently change to CV. Instead, it oscillates between CC and CV.

UNIVERSIDAD PONTIFICIA COMILLAS
ESCUELA TÉCNICA SUPERIOR DE INGENIERÍA (ICAI)
INGENIERO ELECTROMECAÁNICO

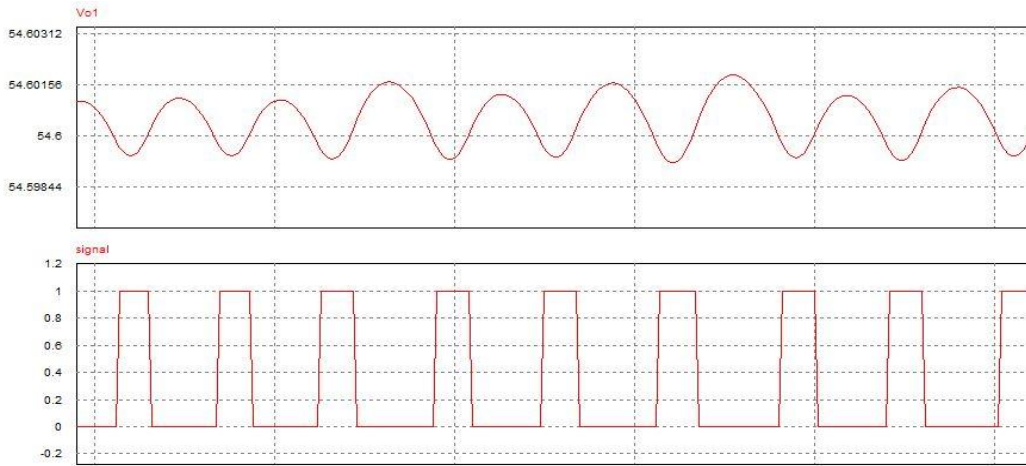


Figure 33: Voltage waveform showing the problem caused when switching from CC to CV.

An ideal comparator would detect whenever the DC component of the voltage output has reached 54.6V and switch only once from CC to CV. This was achieved by using a comparator with hysteresis, shown in Figure 34. This circuit uses two reference values, a high one which is the most important, set to 54.645V (a little more than 54.6V to take into account the ripple), and a small one that will be the one that will be able to change the output once the higher one has been reached. The outputs of the comparators are then connected to a flip flop. The signal that will be used to change from CC to CV is the Q output of the flip flop.

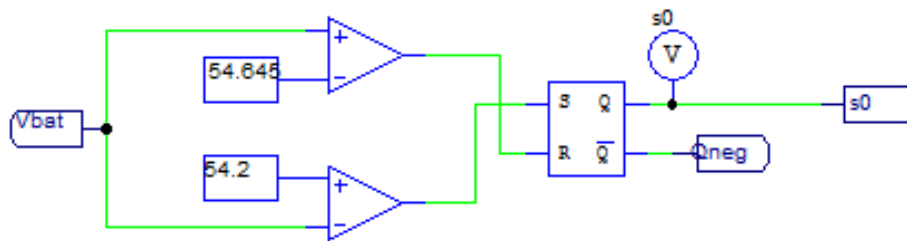


Figure 34: Hysteresis comparator.

All this accuracy is very important since this control will be the one deciding what the full charge battery voltage will be, and as it was mentioned before, a slight overcharge or under-voltage can extremely affect the security and capacity of the battery.

UNIVERSIDAD PONTIFICIA COMILLAS
ESCUELA TÉCNICA SUPERIOR DE INGENIERÍA (ICAI)
INGENIERO ELECTROMECAÁNICO

The simulation in Figure 35 shows how it works, and how it generates only one pulse when the 54.6V voltage is reached. As the voltage rises it first crosses the first reference (54.2V) and nothing happens in the output (Q), although S goes from 1 to 0. Then, when the 54.645V reference is crossed, R changes from 0 to 1, changing at this moment the output Q from 1 to 0, and generating the signal to change from CC to CV. Also, as it can be seen in the simulation, if the voltage drops below 54.645V, the R signal changes from 1 to 0, but the signal that switches from CC to CV remains unchanged.

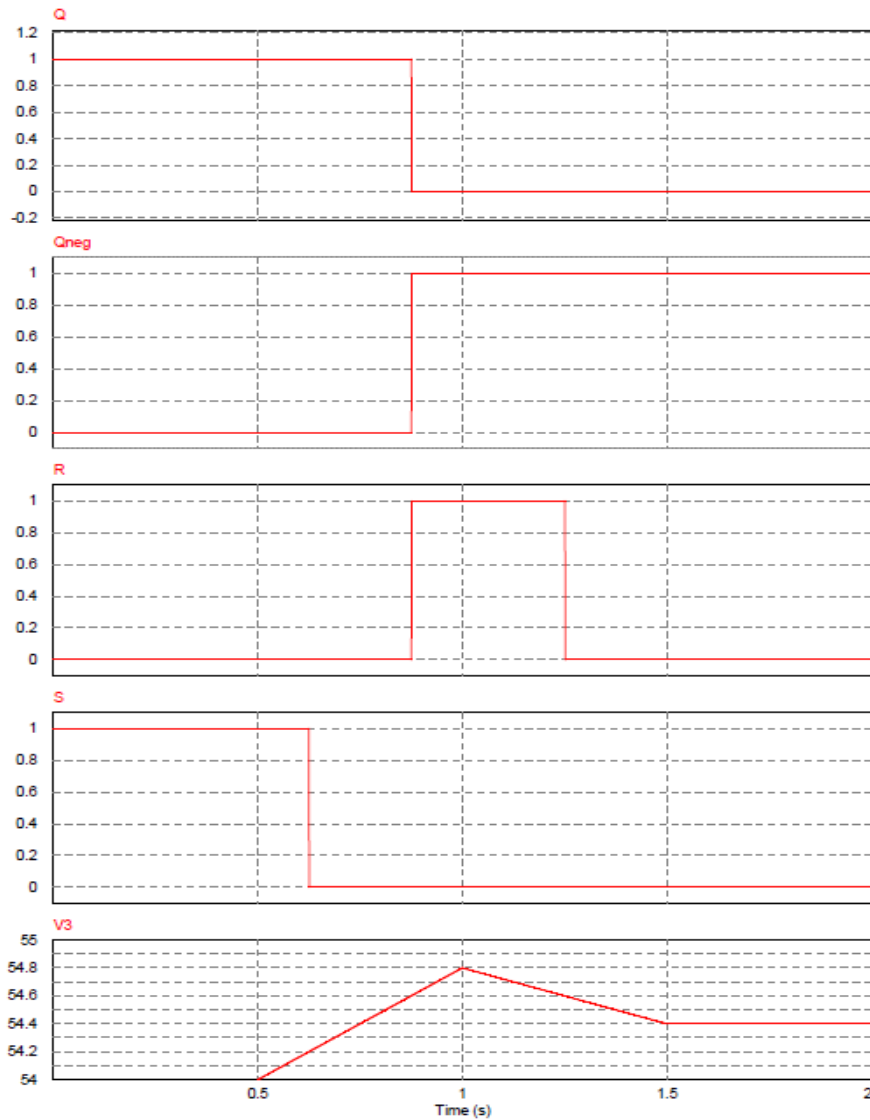


Figure 35: Hysteresis comparator's waveforms.

UNIVERSIDAD PONTIFICIA COMILLAS
 ESCUELA TÉCNICA SUPERIOR DE INGENIERÍA (ICAI)
 INGENIERO ELECTROMECAÁNICO

The next control is the one in charge of finishing the charging process when the battery is fully charged. When the output current drops to 1A during the CV stage, the circuit will send a signal s1 to the multiplexor to change from CV to Finish (duty cycle=0 generated). This is done with a simple comparator. To be more precise, a comparator with hysteresis could have been used, but this control does not require the same accuracy as the one in charge of changing from CC to CV. Also, the problem with the multiplexor going crazy does not happen since, once the 1A limit is reached, the multiplexor sends a duty cycle equal to 0 which opens the switch and the current waveform rapidly drops to 0. Figure 36 shows the simple comparator and signal d2 connected to ground, indicating that the duty cycle will be 0 after the current reaches 1A.

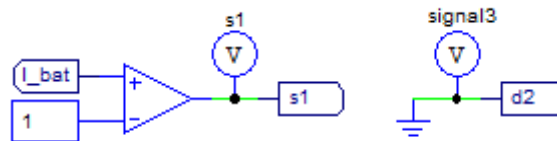


Figure 36: Charge termination control.

Finally, Figure 37 shows the multiplexor which sends the appropriate duty cycle signal to the switch according to the charging stage. Also Table 4 shows the truth table for this multiplexor. Notice that $s1=0$ when $I_{bat}<1A$ and $s0=0$ when $V_{bat}>54.6V$.

s1	s0	Y
X	1	CC (signal1)
1	0	CV (signal2)
0	0	END (signal3)

Table 4: Multiplexor's table of truth

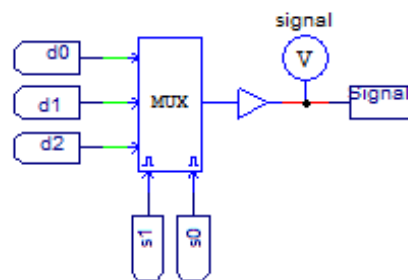


Figure 37: Signal's multiplexor

2.3-6. The input inductor

Finally, to prevent possible electromagnetic interference (EMI) coming from the power supply and also to limit the input current in case a short-circuit occurs in the circuit, a simple $15\mu\text{H}$ inductor has been placed before the full wave rectifier to act as a low pass filter.

2.4- The resulting battery charger

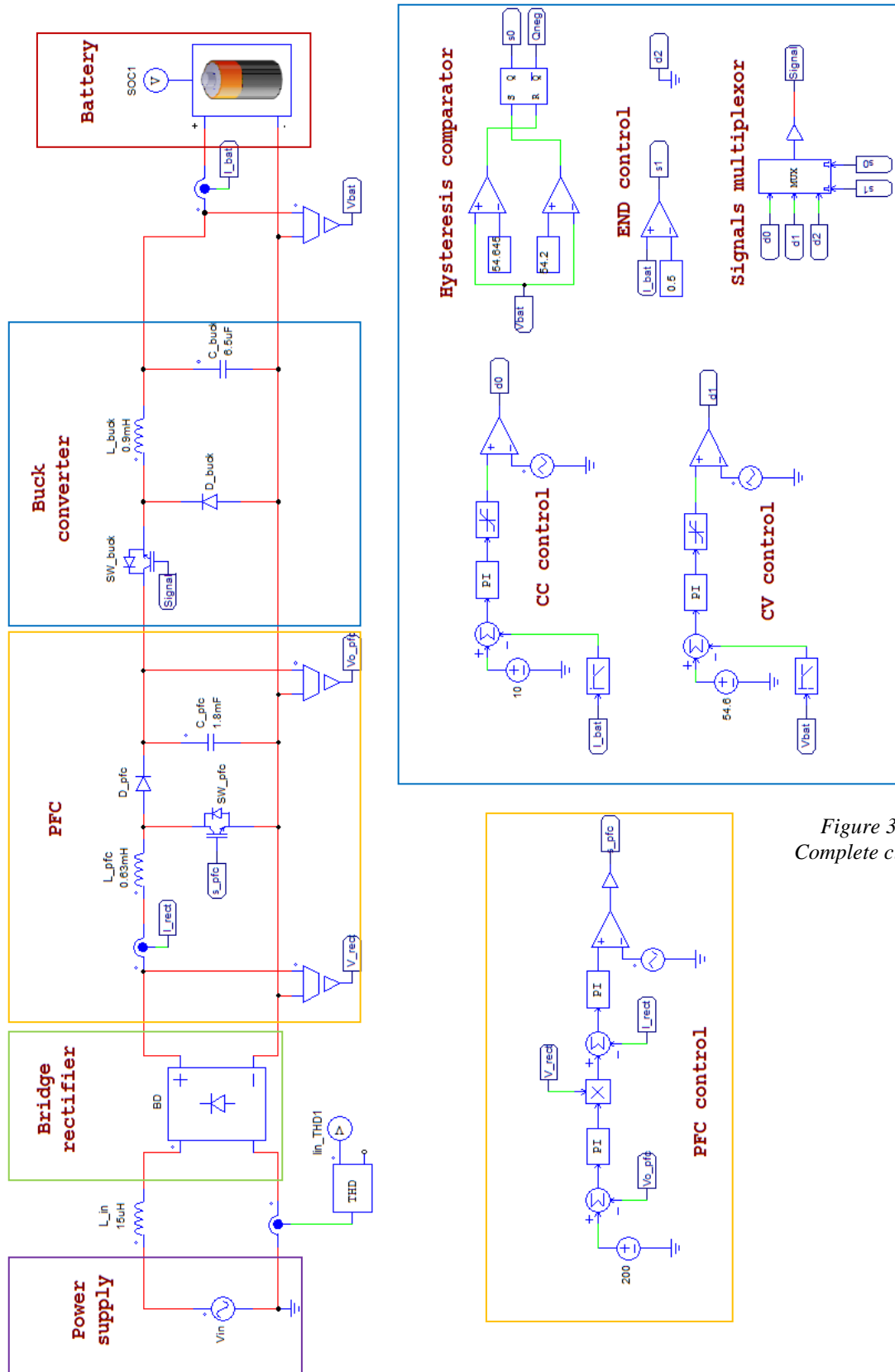


Figure 38:
Complete circuit

Chapter 3: Components

In order to be able to calculate an approximated cost for this design, to calculate more precisely the efficiency of the whole circuit and as the first step in the building of a prototype, the components for this battery charger must be carefully selected to minimize the cost and maximize the efficiency.

Below is a detailed explanation of how and why the different components (transistors, diodes, inductors, capacitors, resistors and microcontroller) have been chosen.

2.5- Transistors

In the circuit there are two transistors that are used as switches: one in the Boost converter used for the power factor correction (PFC) and another one in the Buck converter. In order to choose the appropriate components the switching frequency and maximum currents and voltages are taken into account:

- PFC switch:
 - $V_{\max} = 205\text{V}$
 - $I_{\max} = 9\text{A}$
 - $f_{\text{sw}} = 40\text{kHz}$

- Buck converter switch:
 - $V_{\max} = 205\text{V}$
 - $I_{\max} = 11\text{A}$
 - $f_{\text{sw}} = 40\text{kHz}$

To guarantee a safe operation, the devices will be selected with a wide margin of safety of 100%; that is a rated voltage of 400V and rated current of 20A. Nowadays, there is a great

UNIVERSIDAD PONTIFICIA COMILLAS
 ESCUELA TÉCNICA SUPERIOR DE INGENIERÍA (ICAI)
 INGENIERO ELECTROMECAÁNICO

variety of switch-mode power supply transistors, but the two most popular ones are MOSFETs and IGBTs. Figure 39 shows the boundaries between both devices, based on the breakdown voltage and switching frequency.

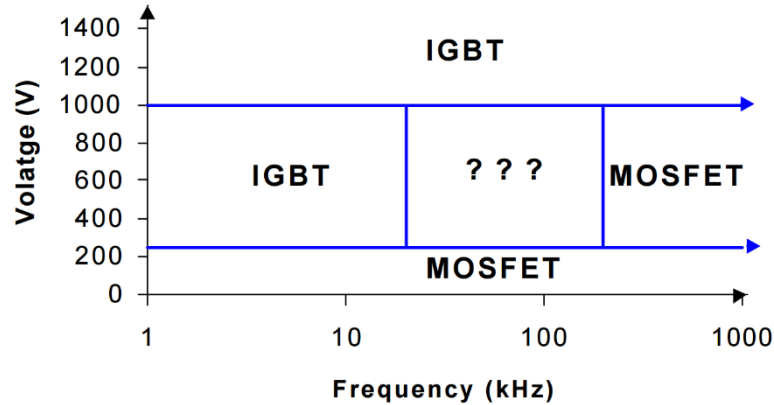


Figure 39: Comparison between MOSFETs and IGBTs.

For this application, the transistors fall in the “cross-over area” where both technologies could be used, so a more detailed study must be done. Table 5 shows the most common conditions under which each technology is used and also typical applications:

Device	Conditions	Applications
IGBTs	<ul style="list-style-type: none"> - Low duty cycle - Switching frequencies under 20kHz - High voltages (over 1000V) - Operation at high junction temperature (more than 100°C) - More than 5kW of output power 	<ul style="list-style-type: none"> - Motor controls - Welding - Air conditions - Electric cars
MOSFETs	<ul style="list-style-type: none"> - Long duty cycle - High switching frequencies (over 200kHz) 	<ul style="list-style-type: none"> - DC/DC converters - Power supplies - Battery chargers

- Low voltage (under 250V)
- Less than 500W output power.

Table 5: Comparison between IGBTs and MOSFETs.

In this case the highest voltage will be of 205V, and the frequency used is relatively fast (40kHz). In this conditions, MOSFETs have greater efficiency than IGBTs, so they are the best option for the battery charger.

There are two main types of MOSFETs: N-channel and P-channel. The N-channel devices have a lower on resistance than P-channel and are cheaper. Also, they require a positive gate-to-source voltage for turn on, which implies some difficulties on the drive. But for applications where the MOSFET is external to the control IC, N-channel devices are preferred for having a better performance and higher efficiency than P-channel.

In consequence, IRFP460 Power MOSFETs will be used for both switches. These transistors are rated for $V_{DSS}=500V$ and $I_D=20A$, and they have an ON resistance of $R_{DS(on)}=0.27\Omega$.

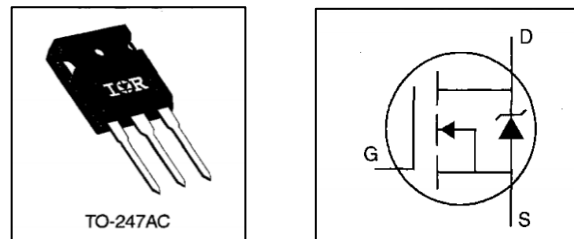


Figure 40: IRFP460 Power MOSFET

2.6- Diodes

The circuit has two diodes (one in the PFC and one in the buck converter) and a diode bridge rectifier. In order to select the two individual diodes the forward voltage drop, breakdown voltage and average forward current will be taken into consideration. The forward voltage drop should be as small as possible. The breakdown voltage should be higher than the

UNIVERSIDAD PONTIFICIA COMILLAS
ESCUELA TÉCNICA SUPERIOR DE INGENIERÍA (ICAI)
INGENIERO ELECTROMECAÁNICO

peak voltage of the circuit and the forward current rating should be above the rms current in the inductor. The diodes will be used in the following conditions:

- Diode_{PFC}: $V_{\max}=205\text{V}$ and $I_{L,\text{PFC}}=5.5\text{A}_{\text{rms}}$
- Diode_{Buck}: $V_{\max}=205\text{V}$ and $I_{L,\text{Buck}}=10\text{A}_{\text{rms}}$

The chosen Diode_{PFC} is a Fairchild Semiconductor FFPF10U40S diode rated for 400V breakdown voltage and 10A average forward current. When operating at 5.5A and 25°C the forward voltage drop is $V_F=1\text{V}$.

For the Diode_{Buck} a Fairchild Semiconductor FFPF20UP40S diode is used, with a rated breakdown voltage of 400V and a rated average forward current of 20A. The forward voltage drop for this diode when operating at 25°C and 10A is $V_F=1\text{V}$.

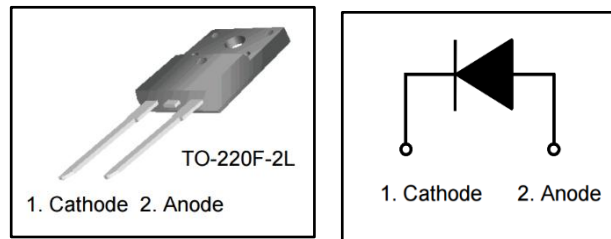


Figure 41: Fairchild Semiconductor FFPF20UP40S

Now, for the diode bridge used as a rectifier, its maximum voltage will be of 170V, which is the peak of the input AC wave, and its peak current will be of 8A.

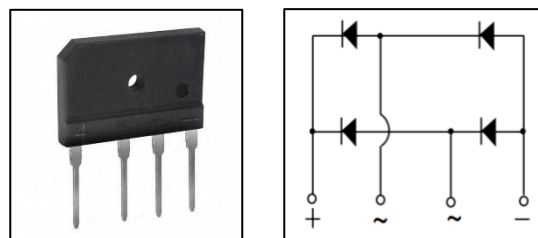


Figure 42: Selected bridge rectifier

2.7- Inductors

There are three inductors in the designed circuit, each one with the following characteristics:

- $L_{in}=15\mu\text{H}$ with a peak current of 8.5A
- $L_{pfc}=630\mu\text{H}$ with a peak current of 8.5A
- $L_{buck}=900\mu\text{H}$ with a peak current of 10.6A

For L_{in} , a $15\mu\text{H}$ fixed inductor with 18A of current saturation, 9.7A current rating and $13\text{m}\Omega$ of DCR will be used.

Now, the other two inductors are quite rare, and buying an industrial component would be expensive (a 0.9mH inductor such as the one used in the buck converter can cost up to \$50). Therefore, the best solution is to design it from scratch, which is common practice among electronic circuit designers. This will take some time, but the cost will be much lower.

There are many white papers on the internet on how to design an inductor such as [12].



Figure 43: Designed inductor.

2.8- Capacitors

In the designed circuit there are two capacitors with the next capacitances, voltage current ratings:

- $C_{pfc}: 1.8\text{mF}$ with 200V.
- $C_{buck}: 6.5\mu\text{F}$ with a maximum voltage of 54.6V.

UNIVERSIDAD PONTIFICIA COMILLAS
ESCUELA TÉCNICA SUPERIOR DE INGENIERÍA (ICAI)
INGENIERO ELECTROMECAÁNICO

Both capacitors will be selected with a rated voltage with a 100% safety margin, so the PFC capacitor will be selected with a rated voltage of 400V and the buck converter's capacitor with a rated voltage of 100V

For the PFC capacitor a United Chemicon aluminum electrolytic capacitor will be used. It has a rated voltage $V_R = 400V$ and an $ESR = 0.15\Omega$.

For the buck converter's capacitor a TS-HA/HB Series Panasonic capacitor will be used. It has a voltage rating of $V_R = 100V$ and an $ESR = 0.08\Omega$.

In order to reduce the ESR effect on the circuit, instead of using a single capacitor, if several capacitors are used in parallel, the equivalent capacitor will have a much lower ESR value.



Figure 44: United Chemicon aluminum electrolytic capacitor.

2.9- Microcontroller

In order to implement the different controls that the circuit has, a microcontroller will be used. In order to select an appropriate microchip, the following specifications for this design were taken into account:

Parameter	Value
A/D channels for the voltage and current measurements	<ul style="list-style-type: none"> - Bridge diode rectifier's output voltage - PFC's input current - PFC's output voltage - Battery's input voltage - Battery's input current <p>Total= 5</p>
PWM generators	2 (PFC and buck)
PWM frequency	40kHz

Table 6: Specifications for the microcontroller.

A PIC24F08KL200 Microcontroller by Microchip was chosen for this design. It has 7 10-bit ADC channels (500k samples per second), 2 Capture Compare PWM (CCP) modules and an 8MHz internal oscillator. A program shall be written in C to make both the PFC and buck closed loops work as they were designed.

UNIVERSIDAD PONTIFICIA COMILLAS
ESCUELA TÉCNICA SUPERIOR DE INGENIERÍA (ICAI)
INGENIERO ELECTROMECAÁNICO

Chapter 4: Costs

In this section, an approximated economical study of the designed battery charger is shown, only taking into account the prices of the different components used in the architecture. This is not an economical study of the final price of the battery charger, since that would include the PCB board, plastic case, labour, PSIM license, etc.

Component	Element	Quantity	Unitary price (\$/unit)	Total cost (\$)
Microchip's PIC24F08KL200 Microcontroller	Closed loop controls	1	1.63	1.63
IRFP460 Power MOSFETs	Buck converter and PFC switches	2	1.60	3.20
Fairchild Semiconductor FFPF10U40S diode	PFC diode	1	1.30	1.30
Fairchild Semiconductor FFPF20UP40S Ultrafast Diode	Buck converter diode	1	1.95	1.95
GBJ1504 15A, 400V Bridge Rectifier	Bridge Rectifier	1	1.33	1.33
PB2020.153NL 15 π H inductor	L_{in}	1	1.87	1.87
Designed inductors	L_{PFC} and L_{buck}	-	-	-
United Chemicon aluminum electrolytic capacitor	C_{PFC}	1	11.12	11.12

UNIVERSIDAD PONTIFICIA COMILLAS
ESCUELA TÉCNICA SUPERIOR DE INGENIERÍA (ICAI)
INGENIERO ELECTROMECAÁNICO

TS-HA/HB Series Panasonic capacitor	C_{buck}	1	6.19	6.19
Resistor kit	Sensors	1	10	10
Total Price= \$38.59				

Table 7: Components and costs.

Chapter 5: Simulations and remarks

In this section, simulations of the different parts of the finished circuit are shown. This will serve as a result for the project, showing how all the individual blocks work as expected, and also how they are integrated well.

In order of position from the power supply to the battery, the following simulations will be shown:

- 1- PFC (including the bridge rectifier).
- 2- PFC controls.
- 3- Buck converter.
- 4- Buck converter controls.

Finally, the resulting simulation of the whole charge process will be shown and explained, showing the voltage and current charge curves of the battery.

2.10- PFC (with bridge rectifier)

As it was explained earlier, the PFC block was introduced to first, increase the power factor to nearly 1, and secondly to deliver a dc voltage to the buck converter. The first simulation (Figure 45) shows the input voltage and current to the final charger before applying the PFC.

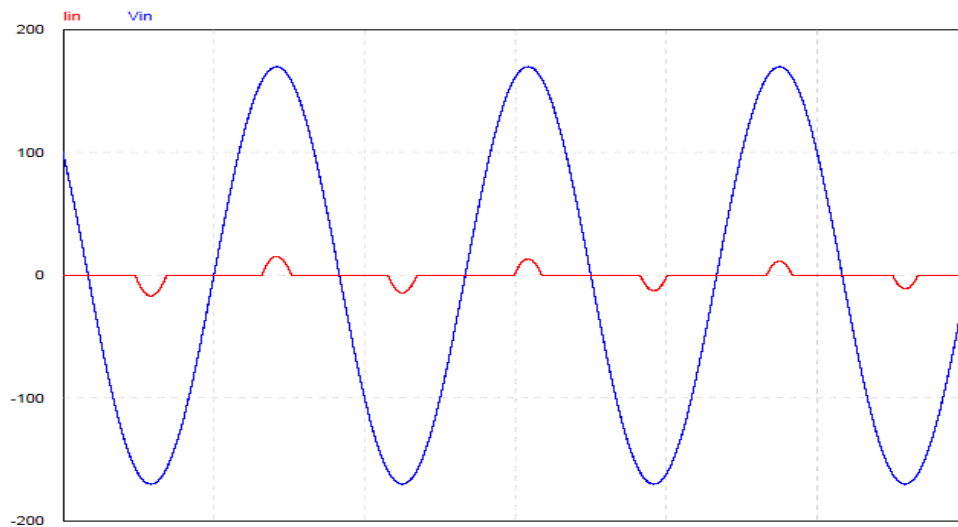
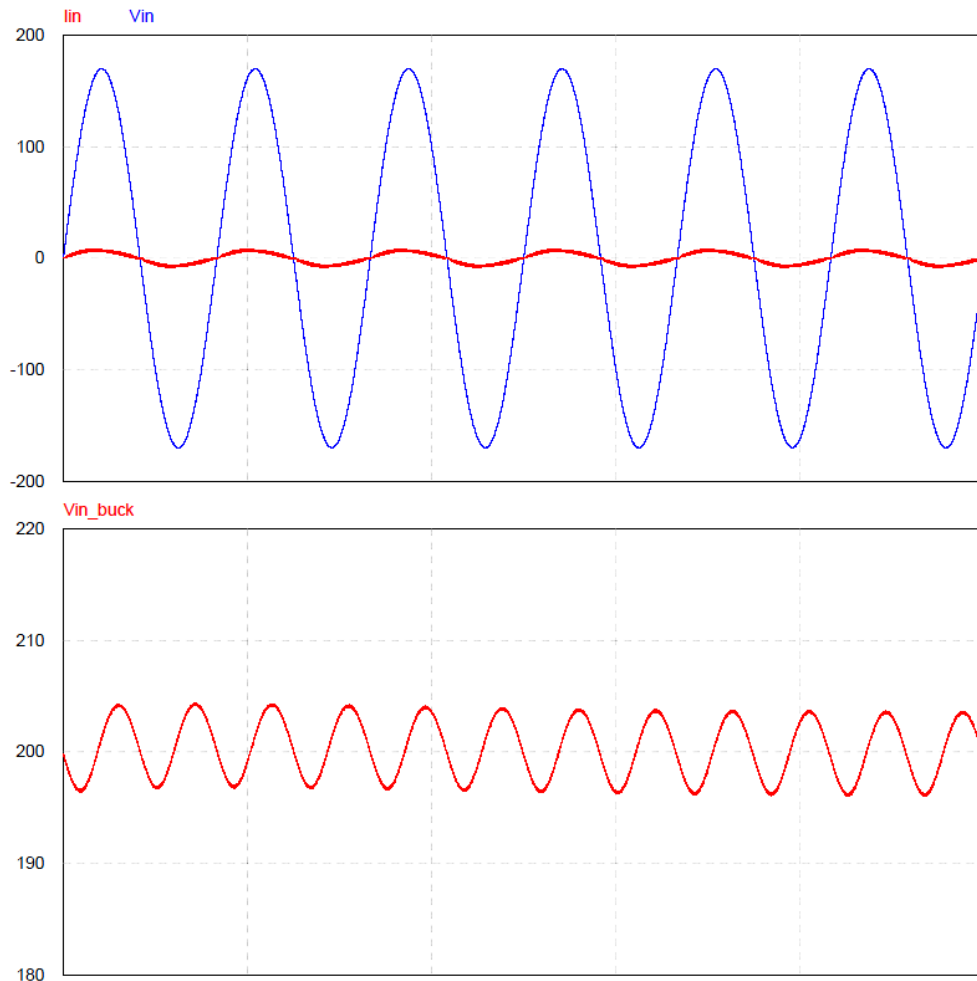


Figure 45: Input voltage and current to the final charger before applying the PFC.

It is clear that without the PFC, the input current is far from being a clean sinusoidal, having a power factor of $PF=0.59$. Without the PFC, this charger would not meet the regulations required for this type of device [8].

Below, Figure 46 shows the same result when the PFC is included in the design. It also shows the PFC's output voltage, which will serve as an input for the buck converter.

UNIVERSIDAD PONTIFICIA COMILLAS
ESCUELA TÉCNICA SUPERIOR DE INGENIERÍA (ICAI)
INGENIERO ELECTROMECAÁNICO



*Figure 46: Above: Input voltage and current to the charger using PFC.
Below: PFC's output voltage.*

Now the current has a much cleaner waveform, being almost sinusoidal and being synchronized with the input voltage. The power factor for the battery charger is now $PF=0.982$, which is very good and perfectly compatible with the regulations.

Also, Figure 46 shows the PFC's output voltage. It is a sinusoidal with a dc component of 200V and a ripple of 10V ($\Delta V_o/V_o = 5\%$) as it was expected.

2.11- PFC controls

The next simulations correspond to the PFC feedback loop (shown in Figure 47). The functioning of this control system was explained earlier so only a simulation of each one signal will be shown with a quick description to understand what is happening from curve to curve.

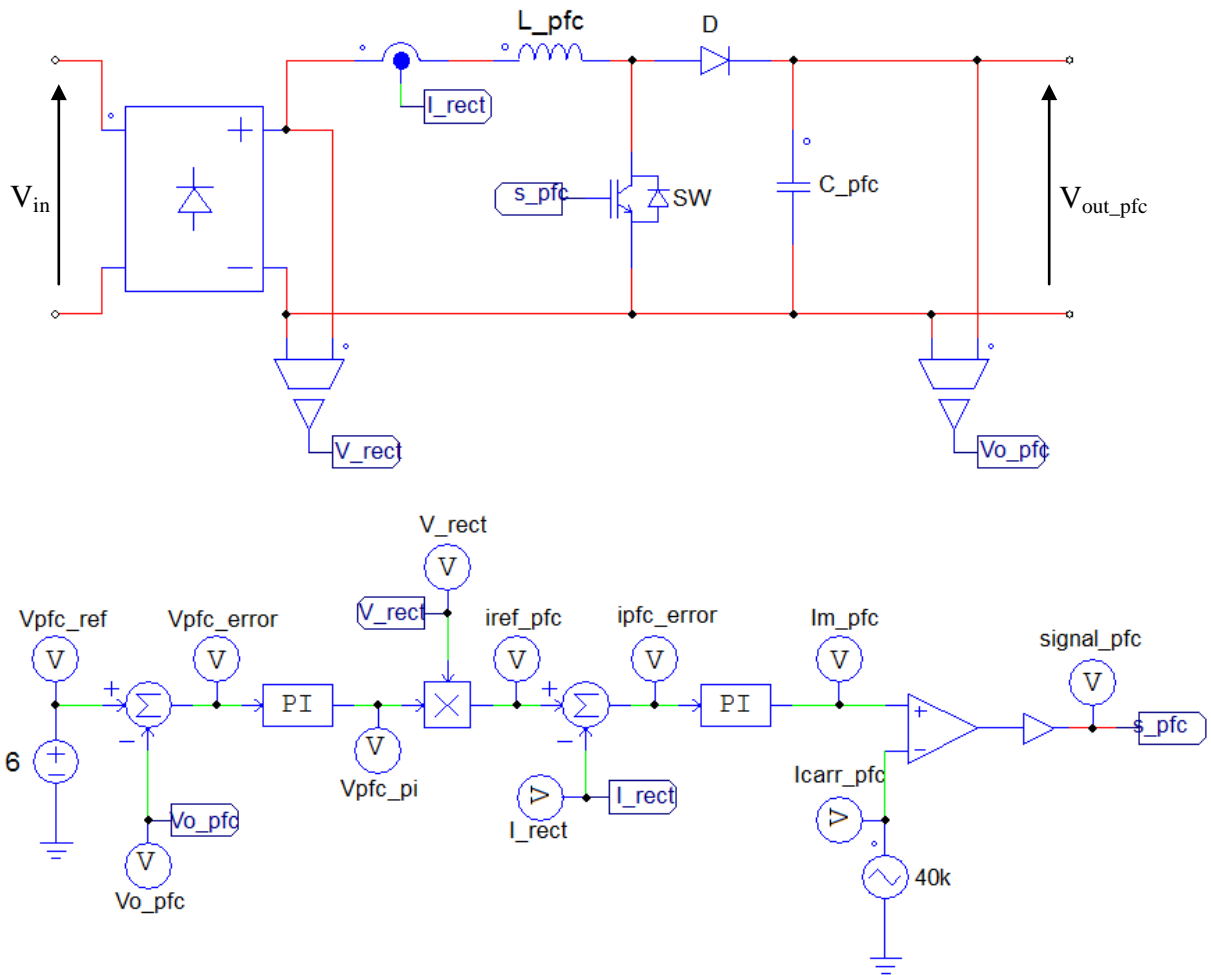


Figure 47: PFC topology with its feedback loop.

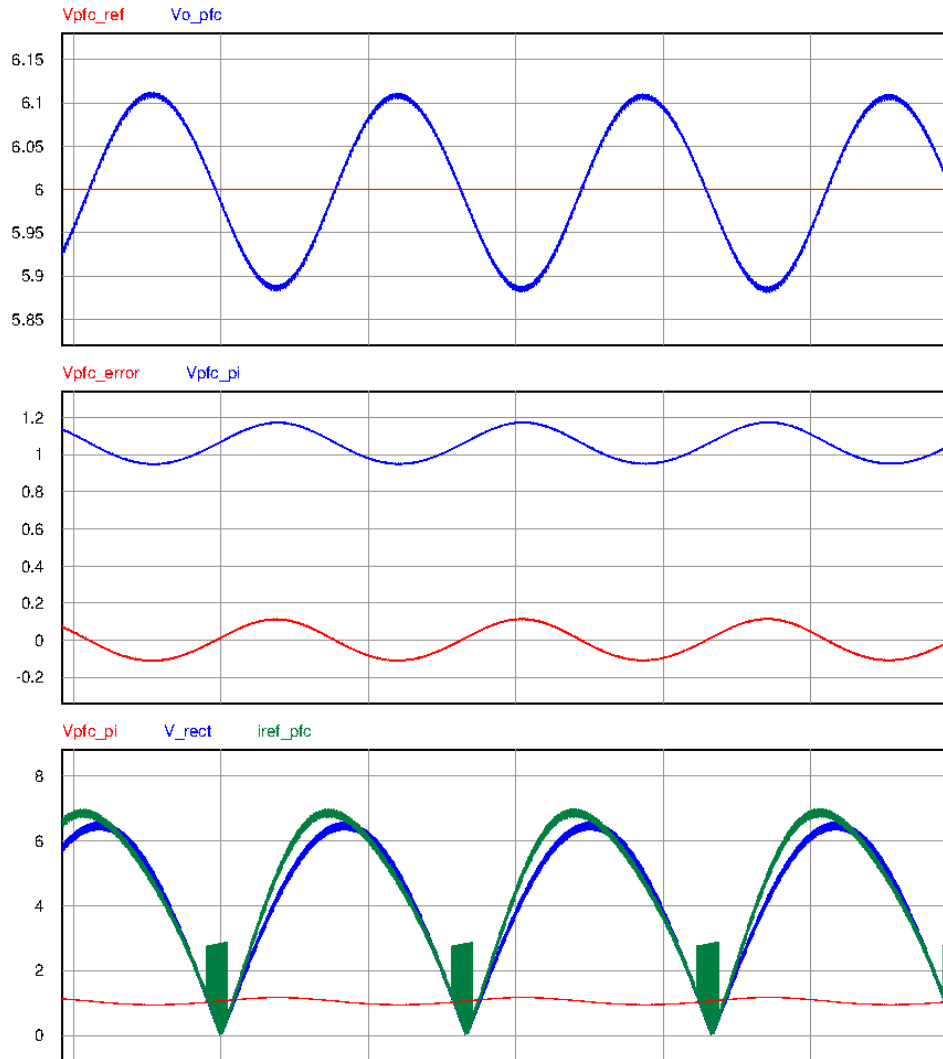


Figure 48: PFC controls' simulations.

Figure 48 shows the different signals in the outer voltage loop. First, the PFC's output voltage V_{o_pfc} is compared to the voltage reference V_{pfc_ref} . The error signal V_{pfc_error} is then multiplied by the PI controller, obtaining V_{pfc_PI} . Then this signal is multiplied by the bridge rectifier's output voltage V_{rect} , obtaining a current I_{ref_pfc} reference which is synchronized with the input voltage waveform. This signal will be the input to the inner current loop, whose signals are shown in the next Figure 49.

UNIVERSIDAD PONTIFICIA COMILLAS
ESCUELA TÉCNICA SUPERIOR DE INGENIERÍA (ICAI)
INGENIERO ELECTROMECÁNICO

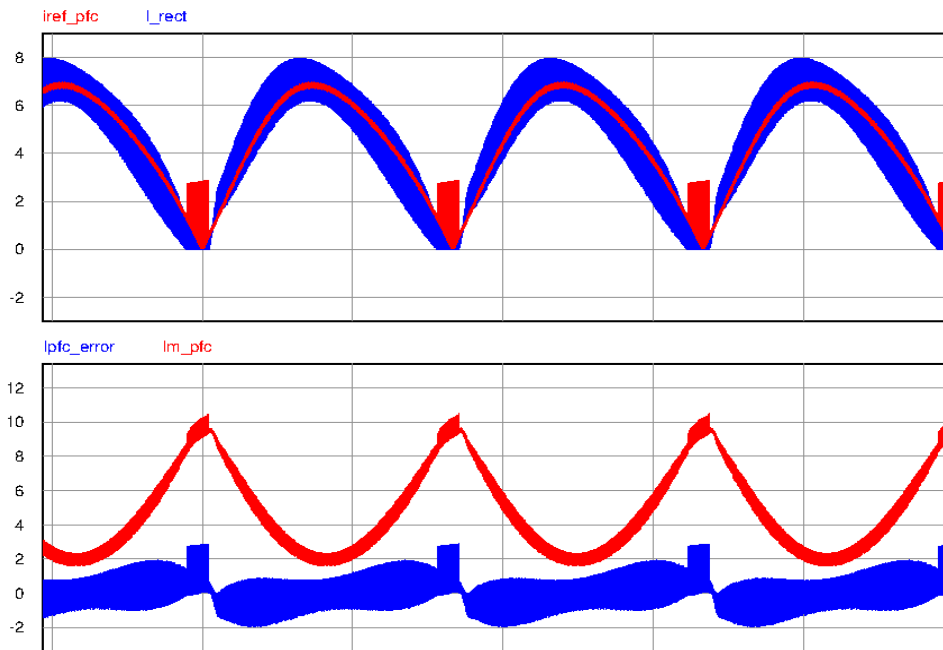


Figure 49: PFC controls' simulations.

Figure 49 shows starts by showing the comparison between the inductor's current reference I_{ref_pfc} and the measured inductor's current. The result is the error signal I_{pfc_error} which after being multiplied by the PI controller results in the waveform I_{m_pfc} .

UNIVERSIDAD PONTIFICIA COMILLAS
ESCUELA TÉCNICA SUPERIOR DE INGENIERÍA (ICAI)
INGENIERO ELECTROMECAÁNICO

At last, as shown in Figure 50 this signal is compared with a sawtooth waveform, generating the duty cycle signal that controls the PFC's switch.

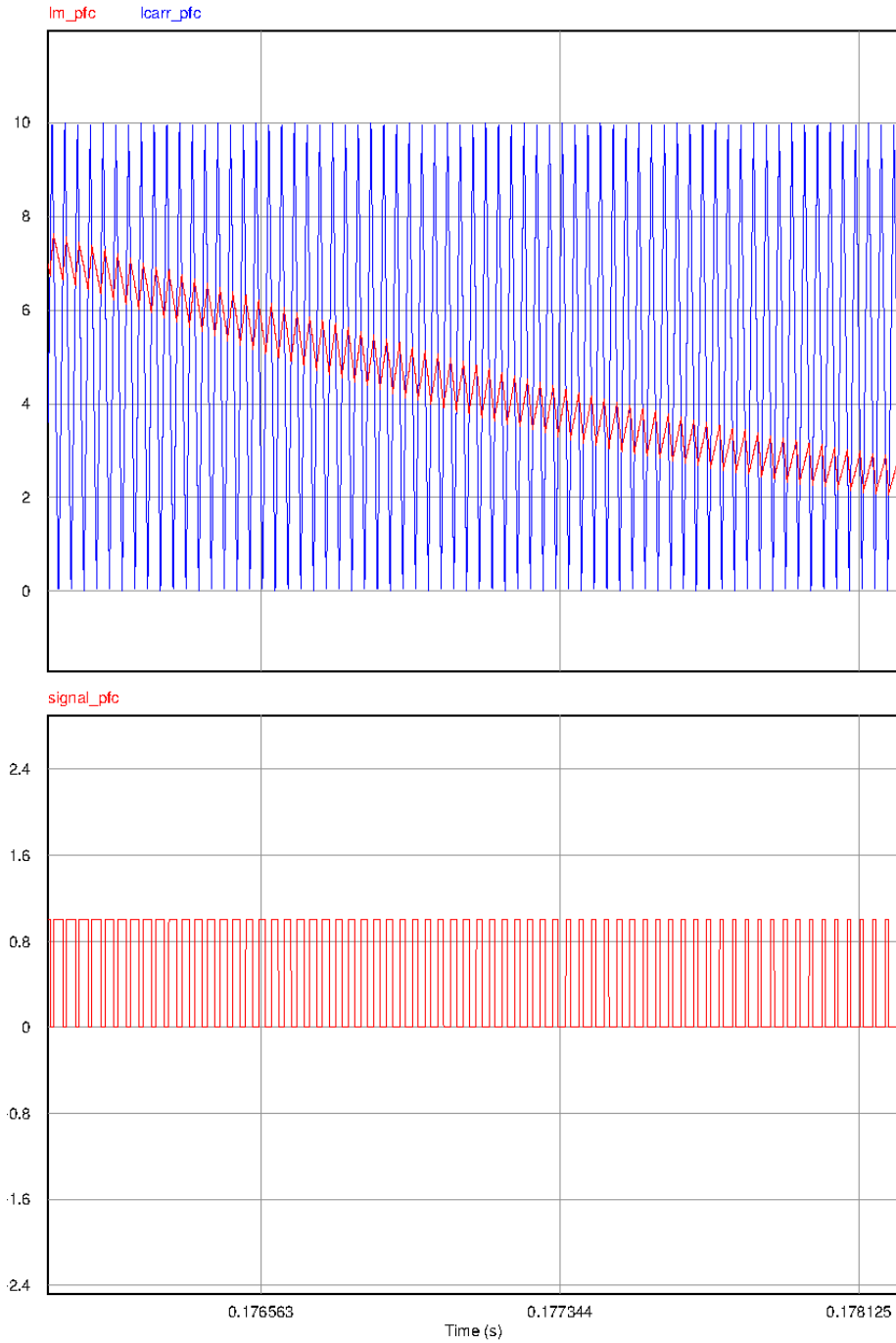


Figure 50: PFC's PWM signal.

2.12- Buck converter

Figure 51 shows the three main waveforms concerning the buck converter. The first one is the PFC's output voltage, which is the input to the buck converter. The next two are the output voltage and output current, directly connected to the battery. It can be seen how the voltage ripple is very small, approximately 0.08V, and the current ripple too, approximately 1A. Also, there are slight fluctuations in the current, which are caused by the PFC's output voltage. These were not considered important.

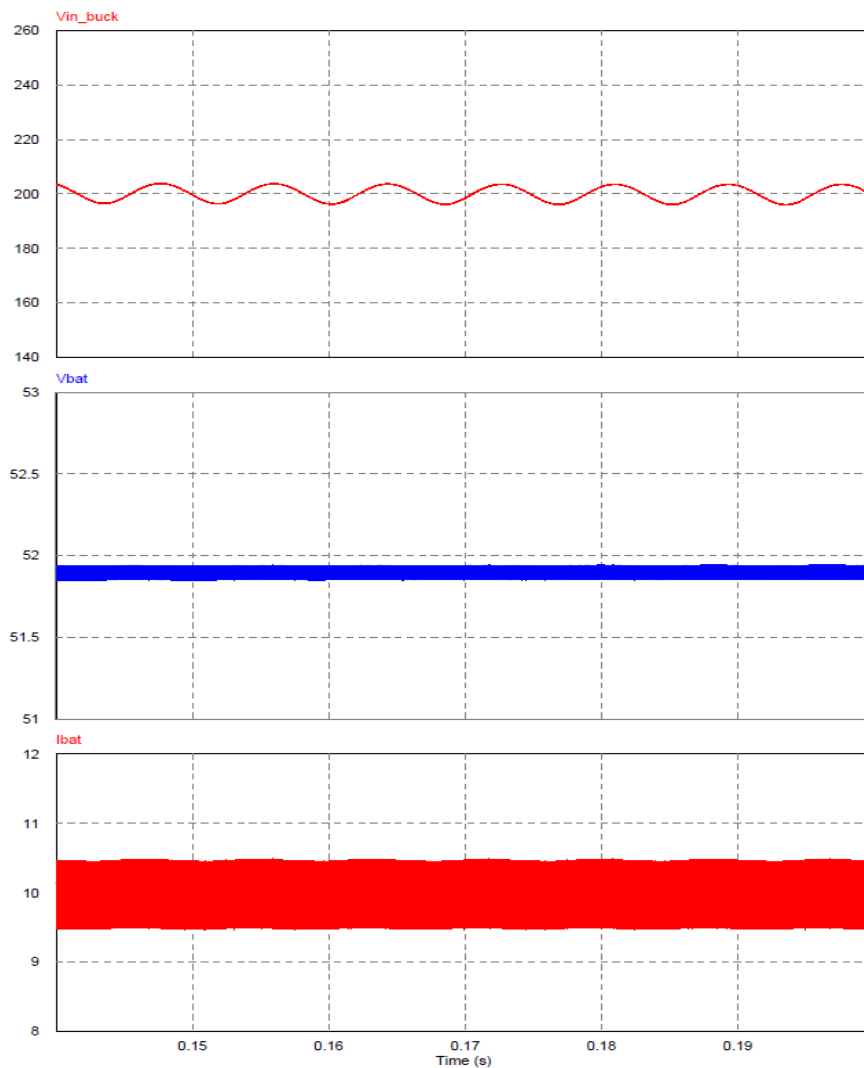


Figure 51: a) PFC's output voltage. b) Buck converter's output voltage. c) Buck converter's output current.

2.13- Buck converter controls

The next pages show the simulations of the buck converter controls both in CC (Figure 52) when SOC=0.7, and in CV (Figure 53) when SOC=0.95.

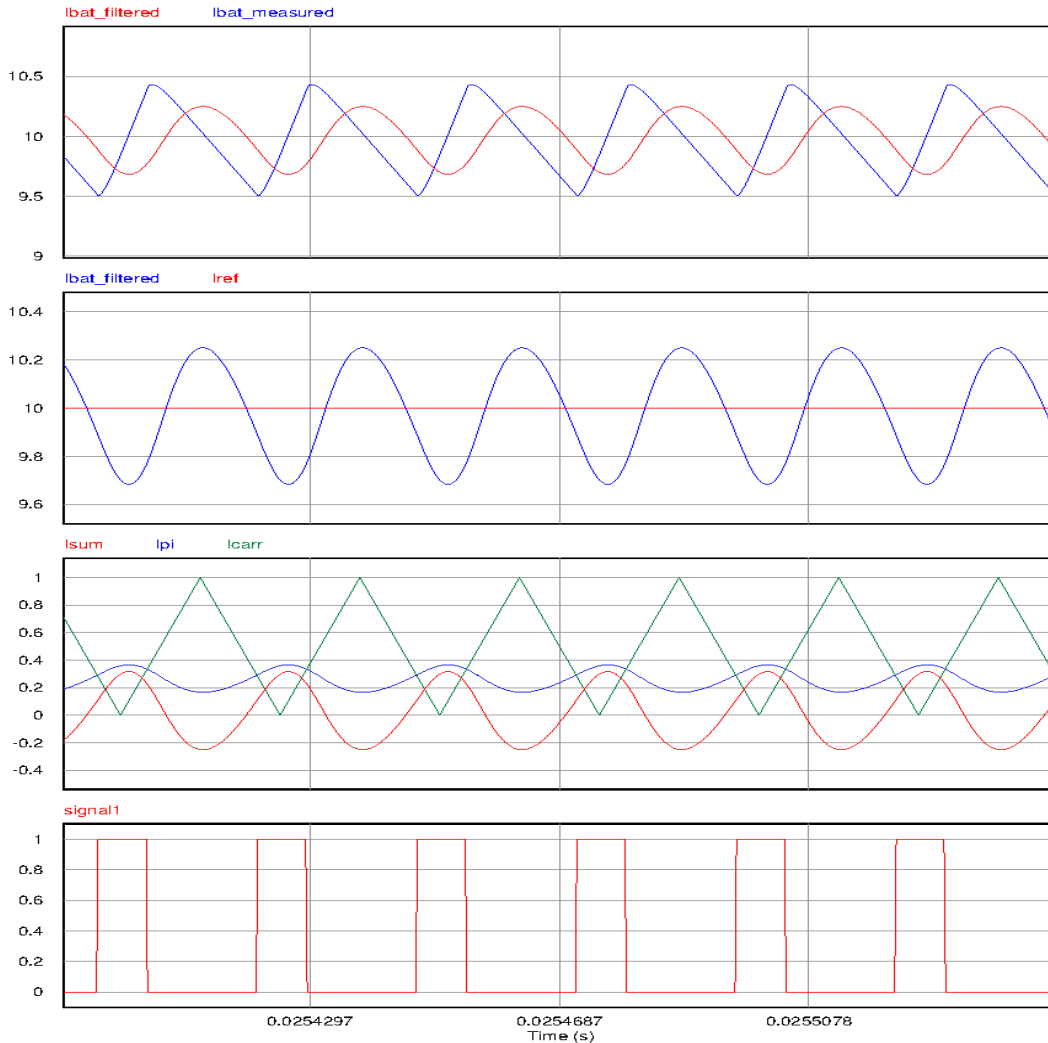


Figure 52: Buck converter's control's signals in CC.

The first simulation shows the measured current before ($I_{bat_measured}$) and after the low pass filter ($I_{bat_filtered}$). This filter was added in the end to make the measured waveform cleaner and easier to control. Then this filtered current is compared to the 10A reference I_{ref} .

UNIVERSIDAD PONTIFICIA COMILLAS
 ESCUELA TÉCNICA SUPERIOR DE INGENIERÍA (ICAI)
 INGENIERO ELECTROMECAÁNICO

The error I_{sum} is multiplied by the PI controller, obtaining I_{PI} . This signal is compared to the 40kHz carrier signal and the final result is the duty cycle signal *signal1*.

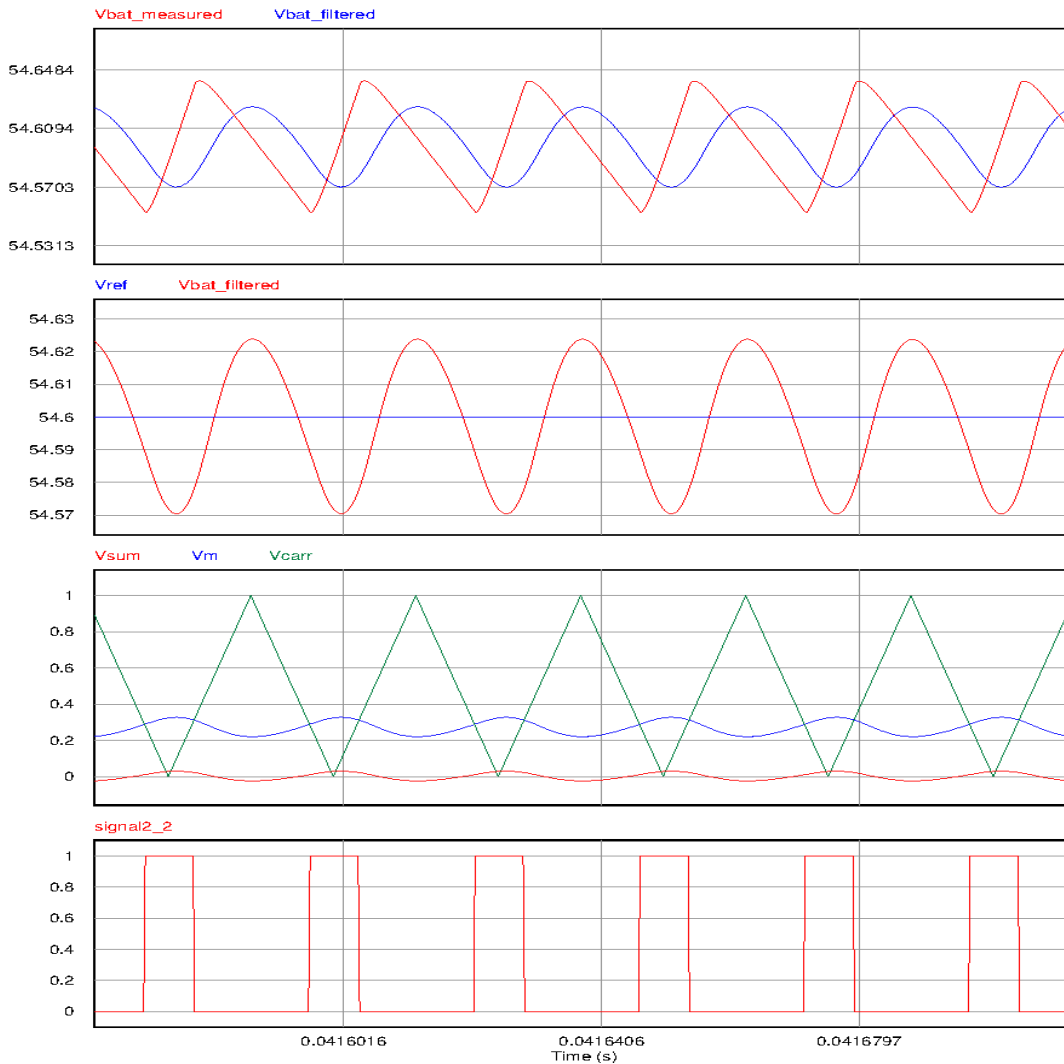


Figure 53: Buck converter's control's signals in CV.

Figure X shows the control signals when the charger is working in CV. The functioning is completely analogous to that of the CC control. The first simulation shows the measured voltage before ($V_{bat_measured}$) and after the low pass filter ($V_{bat_filtered}$). Then this filtered

voltage is compared to the 54.6V reference V_{ref} . The error V_{sum} is multiplied by the PI controller, obtaining V_m . This signal is compared to the 40kHz carrier signal and the final result is the duty cycle signal $signal2_2$.

2.14- Final charging simulation

In this section, the whole battery charge process is shown and analyzed. Due to the fact that the switching frequency is relatively fast (40kHz), and that the battery takes a long time to charge (approximately 2.5 hours), a simulation of the whole charging process would weigh around 30 gigabytes. The computer used for the design was not able to simulate it all, so instead of doing that, several snapshots were taken during the whole charging process, measuring data as the SOC slowly increases. Finally, the data was represented in Excel giving the result shown in Figure X.

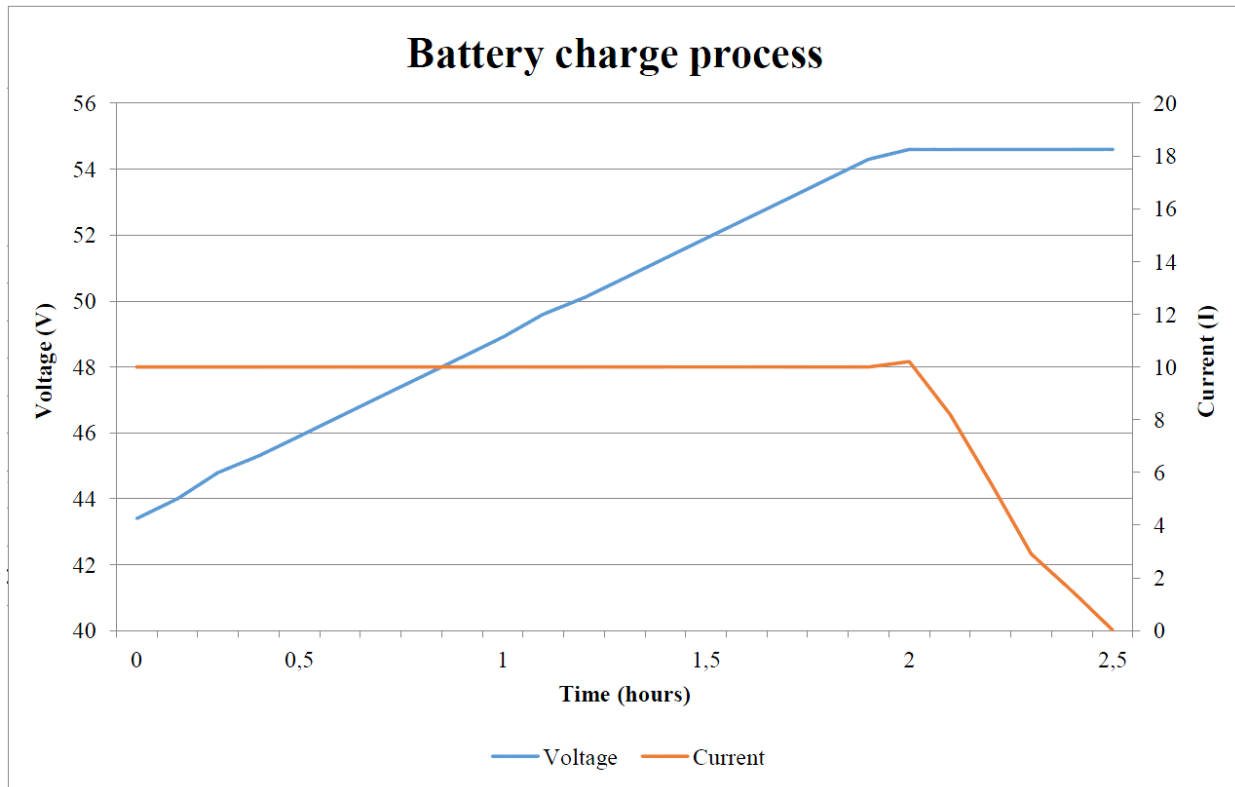


Figure 54: Results of the voltage and current charging curves.

The graph shows the two stages of the battery charging process:

- 1- First, during the Constant Current stage, the charger supplies 10A to the battery and this makes the voltage increase slowly. The resulting voltage curve during this stage resulted very similar to the one shown in Figure 55 for a single LG battery cell being charged at 0.5C (red curve) [2]. This is a good result because it means that the battery pack model was well designed.

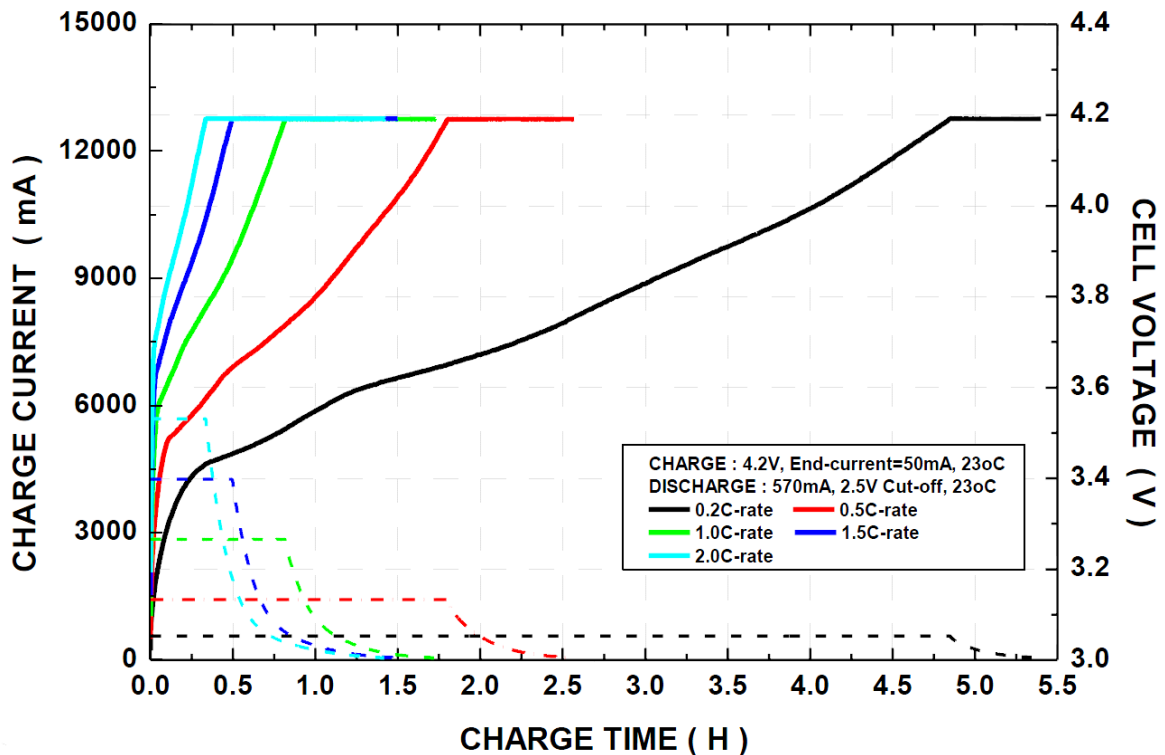


Figure 55: Charging curves for an LG battery cell under several C-rates.

- 2- After two hours of charging, the battery voltage reaches its maximum (54.6V) and the hysteresis comparator detects it, changing the charging method from Constant Current to Constant Voltage. At this moment, the current stops being controlled and a spike in the current occurs, going up to 10.2A, before starting to fall. This could be because the charger

UNIVERSIDAD PONTIFICIA COMILLAS
ESCUELA TÉCNICA SUPERIOR DE INGENIERÍA (ICAI)
INGENIERO ELECTROMECAÁNICO

changes to CV method a bit too early and the voltage has not completely reached 54.6V yet. Hence, at the moment of change, the voltage is suddenly forced to be 54.6V and the battery demands a spike of current to do so. After the voltage is stabilized in 54.6V, the current can start decreasing.

This current spike does not suppose a big concern since the battery is prepared for being charged at higher currents. This design charges the battery at a very conservative 0.5C, so if it goes up a little bit (0.52C), this does not cause any stress to the battery.

Below is a set of charging points taken throughout the process as the SOC increases. Four representative moments of charge are shown:

- 1- Figure 56: SOC=0.1 and the charger is therefore charging in CC.
- 2- Figure 57: SOC=0.95, the charger is charging in CV.
- 3- Figure 58: SOC=1 the battery is fully charged and the process is terminated.

5.5.1- SOC=0.1 (CC)

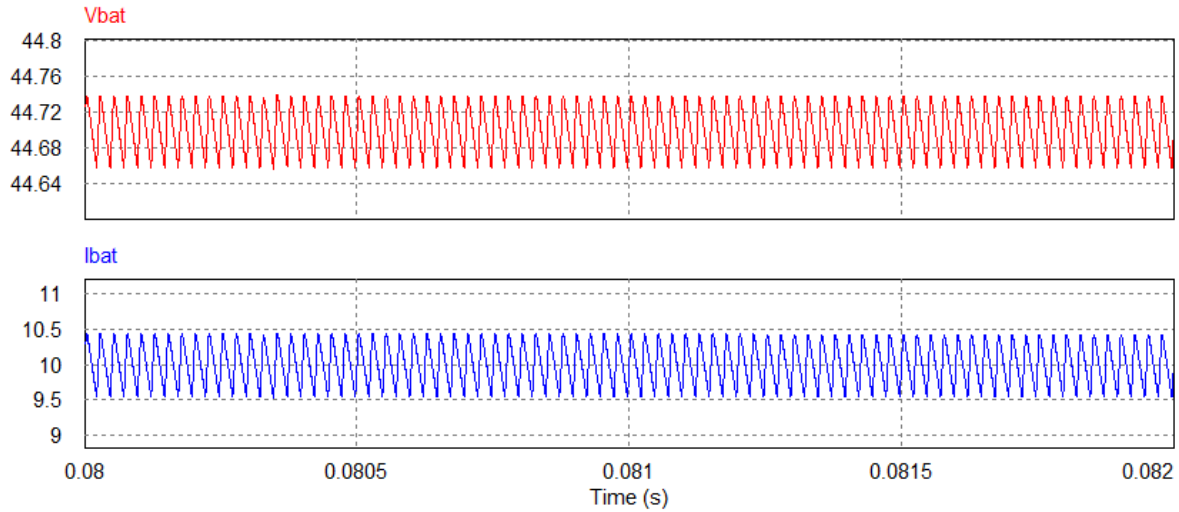


Figure 56: Battery voltage and current curves at SOC=0.1.

Figure X shows how at SOC=0.1, the battery is being charged with a constant current of 10A with a ripple of almost 1A.

It is hard to appreciate because the time span is very short (the computer wouldn't allow for much more due to the size of the circuit), but the voltage is slowly rising, being at this point of about 44.7V with a small ripple of 0.08V.

Both curves appear to be very clean and periodic, with no undesired spikes or changes in the shape. This is because the controls are working well in regulating the current.

5.5.2- SOC=0.95 (CV)

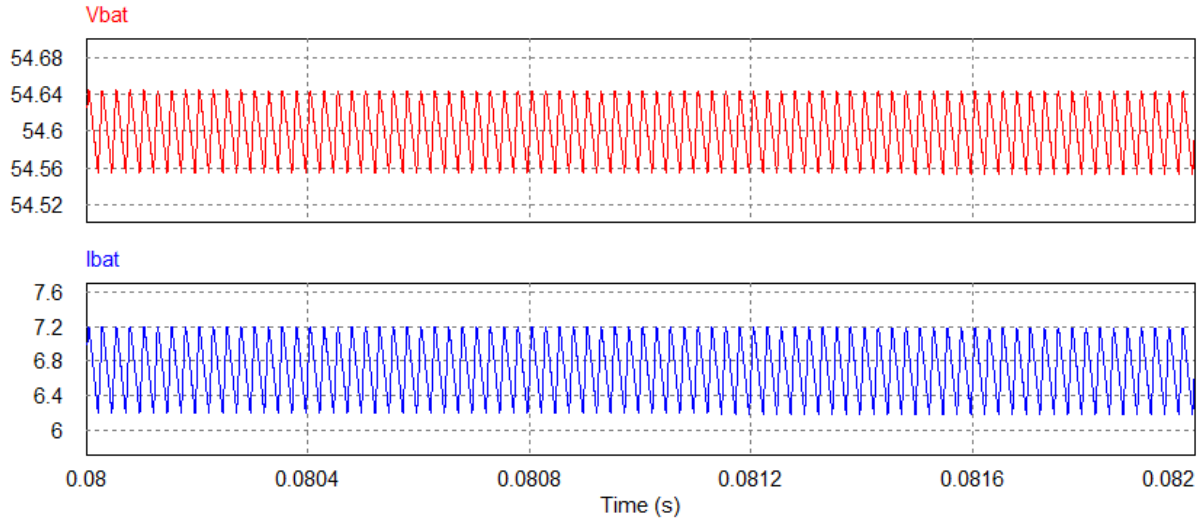


Figure 57: Battery voltage and current curves at SOC=0.95.

Figure X shows the voltage and current being supplied to the battery during the Constant Voltage stage. Here, the charge process is nearly finished and it can be seen how the current is already decreasing (being at this moment around 6.7A its average value).

5.5.3- SOC=1 (Charge complete)

At last, Figure X shows the battery's voltage, current and SOC once the charge is complete.

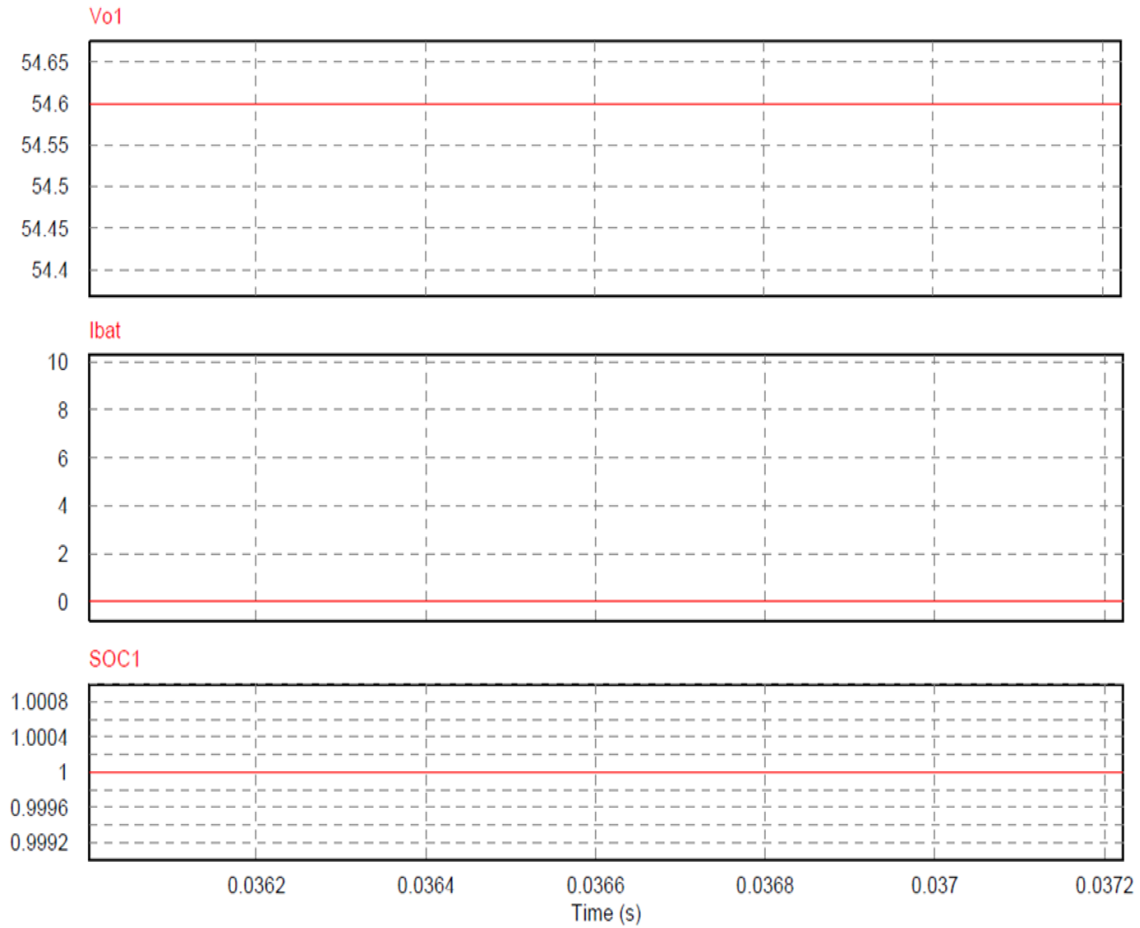


Figure 58: End of charge battery voltage, current and SOC.

Chapter 6: Power efficiency

One of the main objectives when designing an electronic device is maximizing the power efficiency. This is especially true when the device being designed is a battery charger, since they are tremendously used. Making such a popular device save 1 extra watt would end up saving megawatts from the grid. Therefore, if the charger is to be designed taking as a prime objective its efficiency, the following formulas (extracted from [9] and [14]), help the designer identify which components affect the most to the overall efficiency and which internal variables are most related to these losses. In order to do the calculations only the most power consuming elements were taken into account. This will give as a result a power efficiency slightly higher than the one from the real charger if it was to be constructed. But nevertheless, focusing on the main components will give a clear idea of which elements and variables cause the power losses.

Starting from input to output, these are the main power consuming components and their related losses:

Input inductor: $P_{LPFC} = I_{L,rms}^2 \cdot DCR = \left(\frac{8.5A}{\sqrt{2}}\right)^2 \cdot 0.356\Omega = 12.86W$

Bridge diode: $I_{avg} = \frac{2}{\pi} \cdot \frac{\sqrt{2} \cdot P_o}{V_{ac,min}} = \frac{2}{\pi} \cdot \frac{\sqrt{2} \cdot 1000W}{90V} = 10A$

$$P_{bridge} = 2 \cdot I_{avg} \cdot V_{f,bridge} = 2 \cdot 10A \cdot 1.1V = 22W$$

PFC inductor: $P_{LPFC} = I_{L,rms}^2 \cdot DCR = \left(\frac{10.5A}{\sqrt{2}}\right)^2 \cdot 0.175\Omega = 9.65W$

PFC MOSFET: $I_{S1,rms} = \frac{P_o}{V_{ac,min}} \cdot \sqrt{1 - \frac{8 \cdot \sqrt{2} \cdot V_{ac,min}}{3 \cdot \pi \cdot V_o}} = \frac{1000W}{90V} \cdot \sqrt{1 - \frac{8 \cdot \sqrt{2} \cdot 90V}{3 \cdot \pi \cdot 200V}} = 7.53A$

$$P_{S1,cond} = I_{S1,rms}^2 \cdot R_{on} = 7.53^2 \cdot 0.27\Omega = 15.3W$$

PFC diode: $I_{D1,avg} = \frac{P_o}{V_o} = \frac{1000W}{200V} = 5A$

$$P_{D1,cond} = I_{D,avg} \cdot V_{f,D} = 5A \cdot 0.72V = 3.6W \text{ (diode's conduction loss)}$$

$$P_{D1,switch} = 0.5 \cdot V_o \cdot Q_{rr} \cdot f = 0.5 \cdot 200V \cdot 113 \cdot 10^{-9}C \cdot 40 \cdot 10^3Hz = 0.45W$$

$$P_{D1,total} = P_{D1,cond} + P_{D1,switch} = 3.6W + 0.45W = 4.05W$$

UNIVERSIDAD PONTIFICIA COMILLAS
 ESCUELA TÉCNICA SUPERIOR DE INGENIERÍA (ICAI)
 INGENIERO ELECTROMECAÁNICO

$$\text{PFC capacitor: } I_{Co,rms} = \sqrt{\frac{8 \cdot \sqrt{2} \cdot P_o^2}{3 \cdot \pi \cdot V_{ac,min} \cdot V_o} - \frac{P_o^2}{V_o^2}} = \sqrt{\frac{8 \cdot \sqrt{2} \cdot (1000W)^2}{3 \cdot \pi \cdot 90V \cdot 200V} - \frac{(1000W)^2}{(200V)^2}} = 6.46A$$

$$P_{Co} = I_{Co,rms}^2 \cdot ESR = (6.46A)^2 \cdot 0.01\Omega = 0.41W$$

$$\text{Buck converter MOSFET: } I_{S2,rms} = \sqrt{\frac{V_o}{V_{in}} * \left(I_o^2 + \frac{\Delta I^2}{12} \right)} = \sqrt{\frac{54.6V}{200V} * \left(10A^2 + \frac{(1A)^2}{12} \right)} = 5.22A$$

$$P_{S2,cond} = I_{S2,rms}^2 \cdot R_{on} = (5.22A)^2 \cdot 0.27\Omega = 7.35W$$

$$\text{Buck converter inductor: } I_{L,rms} = \sqrt{\left(I_o^2 + \frac{\Delta I^2}{12} \right)} = \sqrt{\left(10A^2 + \frac{(1A)^2}{12} \right)} = 10A$$

$$P_{Lbuck} = I_{L,rms}^2 \cdot DCR = (10A)^2 * 0.175 \Omega = 17.5W$$

$$\text{Buck converter diode: } P_{D2,cond} = V_{f,D} \cdot I_o \cdot \left(1 - \frac{V_o}{V_{in}} \right) = 0.6V \cdot 10A \cdot \left(1 - \frac{54.6V}{200V} \right) = 4.36W$$

$$P_{D2,switch} = 0.5 \cdot V_o \cdot Q_{rr} \cdot f = 0.5 \cdot 54.6V \cdot 138 \cdot 10^{-9}C \cdot 40 \cdot 10^3Hz = 0.15W$$

$$P_{D2,total} = P_{D,cond} + P_{D,switch} = 4.36W + 0.15W = 4.51W$$

$$\text{Total losses: } P_{L,TOTAL} = P_{LPFC} + P_{bridge} + P_{LPFC} + P_{S1,cond} + P_{D1,total} + P_{Co} + P_{S2,cond} + P_{Lbuck} + P_{D2,total} = 12.86W + 22W + 9.65W + 15.3W + 4.05W + 0.41W + 7.35W + 17.5W + 4.51W = 93.63W$$

$$\text{Efficiency : } \eta = \frac{P_o}{P_o + P_{L,TOTAL}} = \frac{1000W}{1000W + 93.63W} \cdot 100\% = 91\%$$

The final efficiency result is 91%. This is a high result, but again, this is only an estimation taking into account the most power consuming elements in the circuit. A prototype would have slightly higher energy consumption.

Chapter 7: Conclusion

In this project, a 48V Lithium Ion battery charger has been designed. In order to do so, several steps have been taken.

First of all, a lot of research was done concerning rechargeable batteries and their charging methods. From all the existing types in the industry, a Lithium Ion battery (AllCell HE-4820) was selected for the battery charger design due to its advantages and extensive use. This type of battery is very fragile so the charging requirements are quite stringent. The charging method used for Li-Ion batteries is the Constant Current Constant Voltage method, and there are several different ways to implement it. The first design step was to decide which sub-circuits would perform this charging method. The first solution for this problem was to use a full wave rectifier to convert the mains power ac voltage to dc and then use a buck converter to step down this voltage to a lower level and control its output current and voltage to perform the CC-CV method.

Before starting with the design of the charger itself, the battery model was designed in PSIM. Due to the lack of information in the AllCell's datasheet, more information was requested to the manufacturer. After obtaining the LG battery cell's datasheet, some parameters were read directly and others had to be obtained through trial and error.

Once this was achieved, the design of the charger commenced. The selection of the component's values was mainly driven by the compromise between the switching frequency and the size of the components. The faster the frequency the smaller the components, but the lower the efficiency. 500kHz is a preferred frequency by many designers to keep a good compromise between size and efficiency, so it was the first frequency used. This posed the first problem, and it is that in order to simulate, the step size must be very small with such a high frequency, making the simulations take as long as hours. This had to be solved by lowering the frequency to a final value of 40kHz, which is still a typical value used in dc-dc converters.

UNIVERSIDAD PONTIFICIA COMILLAS
ESCUELA TÉCNICA SUPERIOR DE INGENIERÍA (ICAI)
INGENIERO ELECTROMECAÁNICO

After finishing the design of the initial charger (full wave rectifier and buck converter with its control system) another problem appeared: this type of devices have very severe regulations in terms of power factor. The charger at this moment had a factor of 0.59, which is far from being acceptable. In order to solve this, a power factor corrector (PFC) was designed and introduced. Again a new problem appeared: to implement the PFC a boost converter was used, and it is forced to step-up the voltage level. In order to keep the charger compatible with both the American and the European voltages ($120V_{ac}$ and $220V_{ac}$ respectively) the voltage had to be stepped-up to $400V_{dc}$. This caused a problem with the buck converters, whose duty cycle would have to be very low to step-down that voltage to the 54.6V used for the battery. This caused errors in the simulations and the only solution was to change the circuit's topology. Finally it was decided to eliminate the compatibility with the European voltage, designing only for the American.

Concerning the controls, the initial design for the isolated converters was not too demanding. The problem came when all the elements were integrated and the ideal components were changed by real components (with ESR and voltage drops). Lots of noise appeared in the controls, making them unable to follow the reference correctly. Two solutions were applied to make the controls work again. First, one of the main problems was caused by the capacitors ESRs being too big, so the solution implemented was to put several parallel capacitors to reduce this series resistance. Secondly, low pass filters were applied after the sensors' measurements in order to eliminate the high frequency noise.

After doing this and slightly adjusting the PI controller values, the control systems started working properly again.

Overall, from all the objectives considered for the present project, only two were unattained:

- As it was mentioned, due to incorrect selection of the dc-dc step-down converter, it was impossible to implement a circuit compatible with the European mains power supply.

UNIVERSIDAD PONTIFICIA COMILLAS
ESCUELA TÉCNICA SUPERIOR DE INGENIERÍA (ICAI)
INGENIERO ELECTROMECAÁNICO

- Also, due to many unexpected problems during the design, the lack of time made it impossible to develop a prototype for the designed circuit.

Nevertheless, the rest of objectives were fulfilled, obtaining a Lithium-Ion battery charger, prepared to fully charge a 48V battery with great accuracy to avoid overcharges. The controls to implement the CC-CV method were well designed, as proved by the clean waveforms shown in the simulations. Also, the charger was designed to attain a great efficiency of 91% and an almost perfect power factor of 0.982, which adequately complies with the existing regulations.

UNIVERSIDAD PONTIFICIA COMILLAS
ESCUELA TÉCNICA SUPERIOR DE INGENIERÍA (ICAI)
INGENIERO ELECTROMECAÁNICO

Chapter 8: Future developments

Even if the proposed battery charger design is already complex and complies with the main charging requirements for a Lithium Ion battery, there are still many things that could be improved in order to make a more sophisticated charger. Some of those improvements are:

- The proposed design has two main problems: the output is not isolated from the input (which may cause safety issues to the battery being charged) and the buck converter's duty cycle limits the range of possible inputs to just the American 120V_{ac}. If instead of a buck converter, a flyback converter was used these two limitations would be removed. The flyback's transformer would not only isolate the output, but it would also allow to provide the 54.6V output with a bigger range of inputs, by adjusting the turns ratio.

The main drawbacks for using a flyback converter are its design complexity and the fact that by using a transformer, the size of the charger would significantly increase. The advantage would be allowing the device to charge the battery safely and from both the American and European voltage levels.

- In order to achieve the most sophisticated charger possible, many more controls should be implemented in order to guarantee the battery's safety and also to maximize the durability of the cells. The following controls could be implemented:
 - If the battery has been over-discharged (its voltage is below 33V), the charger should use a trickle current method to slowly charge it until it reaches 39V, where it is safe to start using the CC-CV method. This is an uncommon situation for Lithium Ion batteries, but nevertheless possible and this would prevent having to discard the battery.
 - Another usefull asset to include in the battery is a battery temperature control. This would permit to end charge if it is being performed on a faulty battery.

UNIVERSIDAD PONTIFICIA COMILLAS
ESCUELA TÉCNICA SUPERIOR DE INGENIERÍA (ICAI)
INGENIERO ELECTROMECAÁNICO

- Also, in order to avoid unnecessary losses, a control system should turn the charger off once the charge is completed. And in addition to this, it should also restart charging automatically if the battery voltage has fallen under a certain value. This would permit having the battery always fully charged without damaging the battery or causing stand-by losses when the battery is not charging.
- Some extra improvements that could refine the charging experience could be to include a state of charge indicator, so the user knows exactly to what extent the battery is charged (many times a complete charge is not needed by the user and a 70% SOC is enough). Also an external button to switch the charger on and off could be useful.
- Finally, a prototype for the designed charger should be implemented to test it and maybe improve some flaws that were not detected in the simulations due to their ideal nature, even though the real model was used in all the components (including series resistances and voltage drops). This would also allow for a more accurate calculation of the efficiency, cost and charging times.

Chapter 9: References

- [1] “AllCell Naked 48V datasheet”, Allcell.
- [2] “Technical Information of LG 18650 MG1”, LG.
- [3] “Accurate, compact, and power-efficient li-ion battery charger circuit”, Min Chen, IEEE.
- [4] “Tutorial how to use lithium ion battery model”, PSIM, PowerSim.
- [5] “BU-409: Charging Lithium-ion”, Battery University.
- [6] “Charging Li-ion Batteries for Maximum Run Times”, Scott Dearborn.
- [7] “Power Electronics”, Daniel W. Hart
- [8] “IEC 61000-3-2 Harmonics Standards Overview”, By Muhamad Nazarudin Zainal Abidin, Schaffner EMC Inc., Edsion, NJ, USA
- [9] “PFC boost converter design guide”, By Sam Abdel-Rahman, Franz Stückler and Ken Siu, Infineon.
- [10] “Power supply HOLD-UP time”, TN0024, Technical note, STMicroelectronics.
- [11] “Fundamentals of Power Electronics. Second Edition”, Robert W. Erickson, Dragan Maksimovic. Univeristy of Colorado. Boulder, Colorado
- [12] “Practical Magnetic Design: Inductors and Coupled Inductors”, Louis R. Diana.
- [13] “Two loop average current control of boost converter”, Dr. Akshay Kumar Rathore, Assistant Professor, National University of Singapore.

UNIVERSIDAD PONTIFICIA COMILLAS
ESCUELA TÉCNICA SUPERIOR DE INGENIERÍA (ICAI)
INGENIERO ELECTROMECAÁNICO

- [14] “Calculating efficiency: PMP-DCDC Controllers”, Arvind Raj, Texas Instruments
- [15] “What’s the best battery”, Battery University, January 11th 2010.
- [16] “Comments on the History of Lithium-Ion Batteries”, Ralph J. Brodd, Broddarp of Nevada, Inc.
- [17] “Battery chargers and charging methods”, Electropaedia.

UNIVERSIDAD PONTIFICIA COMILLAS
ESCUELA TÉCNICA SUPERIOR DE INGENIERÍA (ICAI)
INGENIERO ELECTROMECAÁNICO